DISSERTATIONS IN
FORESTRY AND
NATURAL SCIENCES

Tuomo Silvast

Contrast enhanced computed tomography of articular cartilage

Laboratory investigations on contrast agent molecular mass, charge, concentration and diffusion anisotropy

Publications of the University of Eastern Finland
Dissertations in Forestry and Natural Sciences No 193

UNIVERSITY OF
EASTERN FINLAND

TUOMO SILVAST

Contrast enhanced computed tomography of articular cartilage

Laboratory investigations on contrast agent molecular mass, charge, concentration and diffusion anisotropy

Publications of the University of Eastern Finland
Dissertations in Forestry and Natural Sciences
No 193

Academic Dissertation
To be presented by permission of the Faculty of Science and Forestry
for public examination in the Auditorium SN200 in Snellmania Building
at the University of Eastern Finland, Kuopio, on December, 12^{th} 2015,
at 12 o'clock noon.

Department of Applied Physics

Grano
Jyväskylä, 2015
Editors: Research Director Pertti Pasanen, Prof. Pekka Kilpeläinen,
Prof. Kai Peiponen, and Prof. Matti Vornanen

Distribution:
University of Eastern Finland Library / Sales of publications
julkaisumyynti@uef.fi
http://www.uef.fi/kirjasto

ISBN: 978-952-61-1913-7 (printed)
ISBN: 978-952-61-1914-4 (pdf)
ISSNL: 1798-5668
ISSN: 1798-5668
ISSN: 1798-5676 (pdf)

Author's address: University of Eastern Finland, Department of Applied Physics
P.O. Box 1627
70211 KUOPIO
FINLAND
email: tuomosilvast@gmail.com

Supervisors: Professor Juha Töyräs, Ph.D.
University of Eastern Finland, Department of Applied Physics
Kuopio University Hospital, Diagnostic Imaging Center
P.O. Box 1627
70211 KUOPIO
FINLAND
email: juha.toyras@uef.fi

Professor Jukka Jurvelin, Ph.D.
University of Eastern Finland, Department of Applied Physics
P.O. Box 1627
70211 KUOPIO
FINLAND
email: jukka.jurvelin@uef.fi

Reviewers: Professor Walter Herzog, Ph.D.
University of Calgary, Faculty of Kinesiology
Human Performance Laboratory, KNB 402
2500 University Dr, NW
Calgary, Alberta T2T 1N4
CANADA
email: walter@kin.ucalgary.ca

Docent Mika Koivikko, M.D.
Helsinki University Central Hospital, Department of Radiology
Helsinki Medical Imaging Center
Helsinki
FINLAND
email: mika.koivikko@hus.fi

Opponent: Professor Mika Teräs, Ph.D.
Turku University Hospital, Department of Medical Physics
University of Turku, Institute of Biomedicine
Turku
FINLAND
email: mika.teras@tyks.fi

ABSTRACT

In the early stages of osteoarthritis (OA), the degeneration of articular cartilage involves fibrillation of articular surface and a reduction in the tissue proteoglycan content. In these early stages the disease is difficult to detect with current diagnostic tools such as magnetic resonance and X-ray imaging. However, for optimal management of the disease and development of a more effective treatment, it would be important to achieve a more effective detection of the incipient signs of OA. Contrast enhanced computed tomography (CECT) may represent a promising technique for use in the diagnostics of cartilage injuries and degeneration.

CECT is based on the principle that anionic contrast agents penetrate into the cartilage generally in proportion to the tissue fixed charge density caused by glycosaminoglycans. The difference in X-ray attenuation in contrast enhancement between intact and degenerated cartilage has been proposed as a quantitative measure of the severity of degeneration.

The objective of this study was to evaluate the potential of CECT to detect variations in cartilage composition and integrity. In addition, the effects of contrast agent molecular size, charge, concentration, and diffusion direction on diffusion into articular cartilage were investigated. These issues were studied *in vitro* by using four contrast agents (ioxaglate, gadopentetate, iodide and gadodiamide) and a clinical peripheral quantitative computed tomography (pQCT) scanner.

The X-ray attenuation profile of native cartilage increases from superficial to deep cartilage in agreement with the increasing solid fraction in this direction. In addition, increased diffusion of anionic contrast agent into the superficial layer of articular cartilage reflected proteoglycan depletion of spontaneously degenerated samples. The permeability of the superficial zone is known to increase in early cartilage degeneration, which also contributes to the increased penetration of contrast agent. Diffusion was slower through the deep cartilage than through the articular surface. This indicates

that there is an inverse relationship between the diffusion rate and the tissue solid content. Furthermore, with common clinical contrast agents, the diffusion continued for as long as 24 hours. This implies that in clinical applications, the diffusion equilibrium may not be reached and the diagnostics must be based on imaging at early points of the diffusion. Variations in the concentration of the contrast agent did not affect the diffusion or the interpretation of contrast enhanced images, an important consideration for the clinical applicability of the technique.

To conclude, diffusion equilibrium may not be reached during clinical imaging times before excretion of contrast agent from the joint capsule. The diffusion of substances in articular cartilage depends upon its structure and composition. Proteoglycans are mostly responsible for the distribution of anionic contrast agent in articular cartilage, but also the water content of tissue exerts a significant effect on diffusion in articular cartilage. As long as the limitations of CECT are understood and appreciated during its clinical application, this technique may be capable of imaging of cartilage degeneration *in vivo*.

National Library of Medicine Classification (NLM): QT 36, WE 300, WE 348, WN 160, WN 206
Medical Subject Headings (MeSH): Cartilage, Articular; Diagnostic Imaging; Tomography, X-ray Computed; Contrast Media; Diffusion; Proteoglycans; Osteoarthritis/diagnosis
Yleinen suomalainen asiasanasto (YSA): nivelrusto; kuvantaminen; tietokonetomografia; kontrasti; diffuusio; nivelrikko

Acknowledgements

This study was carried out during the years 2006-2011 in the Department of Applied Physics, University of Eastern Finland.

I want to express my gratitude to the supervisors, professors Juha Töyräs and Jukka Jurvelin, for diverse guidance and comments during this thesis work.

I thank the reviewers of this thesis, professor Walter Herzog and docent Mika Koivikko, for their competent review, comments and suggestions. I want also thank Ewen MacDonald for the linguistic review.

I want especially thank my co-authors Antti Aula, Mikko Lammi, Harri Kokkonen, Thomas Quinn, Miika Nieminen, and Virpi Tiitu for their significant contributions to the studies. The members of the Biophysics of Bone and Cartilage research group, people of the Department of Applied Physics and the SIB Labs Kuopio campus deserve the highest commendations for valuable communication during the years of research and study. The Department of Anatomy and the Kuopio Musculoskeletal Research Unit (KMRU) were invaluable partners in cooperation.

This thesis work was financially supported by Kuopio University Hospital (EVO grants; the Clinical Neurophysiology, the Clinical Physiology and Nuclear Medicine and the Diagnostic Imaging Center), the National Doctoral Programme of Musculoskeletal Disorders and Biomaterials (TBDP), the Sigrid Juselius Foundation and the Aleksanteri Mikkosen säätiö. Without the financial backing this dissertation would have never materialized.

I want to express my dearest thanks to my beloved wife Tuija for patience and understanding, and for my son Mikko for being always so happy and bright.

Toivala, October 2015

Tuomo Silvast

LIST OF PUBLICATIONS

This thesis consists of the present review of the author's work in the field of contrast enhanced tomography of cartilage and the following selection of the author's publications:

I T.S. Silvast, J.S. Jurvelin, A.S. Aula, M.J. Lammi and J. Töyräs, "Contrast agent-enhanced computed tomography of articular cartilage: association with tissue composition and properties", *Acta Radiologica* **50**:1, 78–85 (2009).

II T.S. Silvast, J.S. Jurvelin, M.J. Lammi and J. Töyräs, "pQCT study on diffusion and equilibrium distribution of iodinated anionic contrast agent in human articular cartilage – associations to matrix composition and integrity", *Osteoarthritis and Cartilage* **17,** 26–32 (2009).

III T.S. Silvast, H.T. Kokkonen, J.S. Jurvelin, T.M Quinn, M.T. Nieminen and J. Töyräs, "Diffusion and near-equilibrium distribution of MRI and CT contrast agents in articular cartilage", *Physics in Medicine and Biology* **54,** 6823–6836 (2009).

IV T.S. Silvast, J.S. Jurvelin, V. Tiitu, T.M. Quinn and J. Töyräs, "Bath concentration of anionic contrast agent does not affect their diffusion and distribution in articular cartilage *in vitro*", *Cartilage* **4**:1, 42–51 (2013).

Throughout this thesis, these papers will be referred to by Roman numerals. The original articles have been reproduced with permission of the copyright holders.

AUTHOR'S CONTRIBUTION

The publications selected in this dissertation are original research papers on contrast enhanced computed tomography (CECT).

In all papers I–IV, the author conducted the analysis and interpretation of the CECT data, and was the principal author of the manuscript. In papers I–II, the author conducted the acquisition of the CECT data, and in papers III–IV, the author conducted or supervised the acquisition of the CECT data. In paper I, Antti Aula performed the diffusion rate measurements. In paper III, Harri Kokkonen contributed to the image analysis. In paper IV, Katariina Kulmala calculated the diffusion coefficients.

In all papers, the co-operation with the co-authors has been significant.

ABBREVIATIONS

2D	2-dimensional
3D	3-dimensional
CA	contrast agent
CBCT	cone beam computed tomography
CECT	contrast enhanced computed tomography (contrast enhanced cartilage tomography)
CT	computed tomography
dGEMRIC	delayed contrast enhanced magnetic resonance imaging of cartilage
dQCT	delayed quantitative computed tomography
ECM	extracellular matrix
EDTA	ethylene diamine tetra-acetic acid
EPIC-μCT	equilibrium partitioning of an ionic contrast agent via micro-computed tomography
FCD	fixed charge density
FE	finite element (modeling)
FMC	femoral medial condyle
GAG	glycosaminoglycan
microCT	micrometer scale computed tomography
MR	magnetic resonance
MRI	magnetic resonance imaging
OA	osteoarthritis
PBS	phosphate buffered saline
PG	proteoglycan
pQCT	peripheral quantitative computed tomography
SD	standard deviation
TEO	Terveydenhuollon oikeusturvakeskus (now Valvira, Sosiaali- ja terveysalan lupa- ja valvontavirasto)
TMP	tibial medial plateau
WHO	World Health Organization

SYMBOLS

a_i, a_j	chemical activity
A	area
A, B, S, T	reactants and products in a chemical reaction
$\alpha, \beta, \sigma, \tau$	stoichiometric coefficients
ν_i, ν_j	stoichiometric coefficients
C, c	concentration
D	diffusion coefficient
E	electrical potential
F	Faraday constant, 96 485.3365 C mol^{-1}
Fo	Fourier number
J	diffusive flux
L	length
M	molar mass
n	number of samples
p	p-value of a statistical test
q	charge
Q_r	reaction quotient
r	correlation coefficient
R	molar gas constant, 8.314 4621 J $mol^{-1}K^{-1}$
t	time
T	absolute temperature
x	distance
$\{X_t\}$	instantaneous activity of an ion X
z	number of moles of electrons

Contents

1 Introduction

The use of contrast agents in X-ray imaging of knee was first described in 1931 [1]. Since then, contrast agents have been used in radiographic imaging to enhance the determination of cartilage thickness and morphology. However, contrast agent diffusion in articular cartilage was first measured in 1990 [2]. In that *in vitro* study with human osteochondral samples, nonionic iodinated contrast agent was applied and radiographs were taken over a period of 90 minutes. It was found that contrast agent diffused into osteoarthritic cartilage faster and at a higher concentration than in intact cartilage. In 1996, a delayed gadolinium enhanced magnetic resonance imaging (dGEMRIC) technique which allowed the determination of proteoglycan (PG) distribution in cartilage was introduced [3]. This method is based on the assumption that mobile negatively charged contrast agent molecules distribute in inverse proportion to the local fixed charge density (FCD), which in turn corresponds to the PG distribution of articular cartilage. Ten years later, the first reports on contrast enhanced X-ray tomography of cartilage using a microCT (micrometer scale computed tomography) were published [4, 5]. Subsequently, numerous publications have detailed improvements in contrast enhanced CT imaging of cartilage. Recently, the technique was successfully applied in human knee joint *in vivo* [6,7].

The main functions of articular cartilage are to ensure the smooth movement of the joint through lubrication and the cushioning of mechanical forces impacting on a joint. Articular cartilage is an elastic and layered tissue, tightly connected to the subchondral bone. Approximately three quarters of cartilage weight is attributable to interstitial water [8, 9] with the rest being mainly composed of collagens, proteoglycans and chondrocytes [10].

The first degenerative changes in structure and composition, and in mechanical properties of articular cartilage take place before

they are visually observable [9, 11, 12]. These early degenerative changes in articular cartilage include a decrease in the PG content, fibrillation of the articular surface, breaks in collagen fibrillar network and an increase in the water content [9, 11, 13]. Typically the degeneration begins with the fibrillation of articular surface and the loss of PGs, which consequently leads to an increase in the water content. Although PG loss can be reversible [14], the fibrillation and damage to the collagen network are believed to be irreversible [11]. However, increased synthesis of collagen in osteoarthritic articular cartilage has been reported [15–17]. The PG loss softens cartilage and exposes it to further damage, which can eventually cause a failure of the joint to function properly. In addition, cartilage overloading may cause local injuries that can lead to post-traumatic osteoarthritis (OA) [18]. Since articular cartilage is aneural, the tissue degeneration can be asymptomatic until the damage reaches subchondral bone [19].

At present, in global terms, osteoarthritis is the most common joint disease in adults [20] with over 40 million people suffering a disability caused by this disease [21]. The World Health Organization (WHO) has estimated that nearly 30% of the population over 60 years have symptomatic osteoarthritis [22]. However, the fundamental cause of osteoarthritis is still unclear [20, 23]. In clinical terms, osteoarthritis is believed to represent a heterogeneous group of conditions that leads to joint symptoms. These conditions may involve cartilage, the underlying bone, joint ligaments and muscles, joint capsule, and the synovial membrane [24, 25]. The pathological evolution of knee osteoarthritis may take several years to develop [18]. The first sign suggestive of cartilage damage is often pain on movement [20]. The symptoms of advanced osteoarthritis may involve persistent joint pain or stiffness, joint locking, restricted movements and a limited ability to function [23, 26, 27].

The common treatments for osteoarthritis are pain alleviation with drugs, surgical cartilage repair with either marrow stimulation or a cartilage transplant, or as a last resort, a replacement with an artificial joint [20]. Today, the two most recommended ways to

prevent cartilage degeneration are moderate physical exercise and a reduction of overweight [28]. However, a key element in optimal patient management is early detection. Early diagnosis of osteoarthritis could enable prompt treatment, reduction of future pain and disability, and thus an improvement in the patient's quality of life [29]. In this respect, a sensitive and easy to perform diagnostic tool for PG loss would be highly valuable since it could assist in effective prevention of the progression of the disease. In plain radiography, cartilage is almost transparent. Therefore, a minor tissue loss or marginal superficial changes, which are the initial degenerative changes in cartilage, may well remain undetected [30, 31]. However, these degenerative changes may be visualized with contrast enhancing techniques [5, 32, 33].

In this thesis, the radiological diagnostics of osteoarthrosis was the main focus as well as evaluating the potential of contrast enhanced X-ray tomography of cartilage. Specifically, the diffusion rates and equilibrium distributions of various contrast agents in articular cartilage have been investigated. In addition, the effects of contrast agent and cartilage properties on diffusion were studied. The methodological approach involved studying these parameters in cartilage discs, as well as with osteochondral cylinders *in vitro* using a clinical pQCT (peripheral quantitative computed tomography) scanner.

In the following chapters, the structure, composition and properties of articular cartilage, diagnostics of cartilage degeneration, and contrast agent diffusion in articular cartilage will be described.

2 Articular cartilage

2.1 STRUCTURE AND COMPOSITION

Articular cartilage is an elastic and layered tissue tightly connected to the subchondral bone [34]. It is glassy, with a glistening and bluish white appearance [35]. There are no nerves or blood vessels or lymphatic system within articular cartilage. For this reason, nutrients for chondrocytes are believed to be transported mainly by diffusion and to pass along fluid flows induced by the pressure changes related to joint movements [36]. The thickness of human articular cartilage varies typically between 1 and 4 mm in large joints [37, 38], but for example in the finger joints, its thickness is only 0.5 mm or even less [39].

Articular cartilage can be structurally divided into four layers: superficial layer, middle zone, deep zone, and the calcified cartilage (Figure 2.1). The superficial layer (5–8% of the thickness [40]) consists of densely packed fine collagen fibrils oriented in parallel to the articular surface. The collagen and water contents are higher in the superficial layer than in the other layers. Chondrocytes are flattened and exhibit an ellipsoid shape in the superficial layer [41]. The chondrocyte density is higher than in the other zones, but their biological activity is lower in comparison with the chondrocytes in the deeper zones [42].

In the middle zone (10% of the thickness), the collagen orientation is changing from parallel to vertical direction. The collagen content is slightly lower than in the superficial layer, whereas the PG content may be doubled [35]. In this zone, the chondrocytes are spherical in shape.

In the deep zone (75–80% of the thickness), collagen fibrils are oriented vertically with respect to the articular surface. The water content is lower and the PG content is higher than in the upper layers. Near to the calcified zone there is a slight reduction in the PG

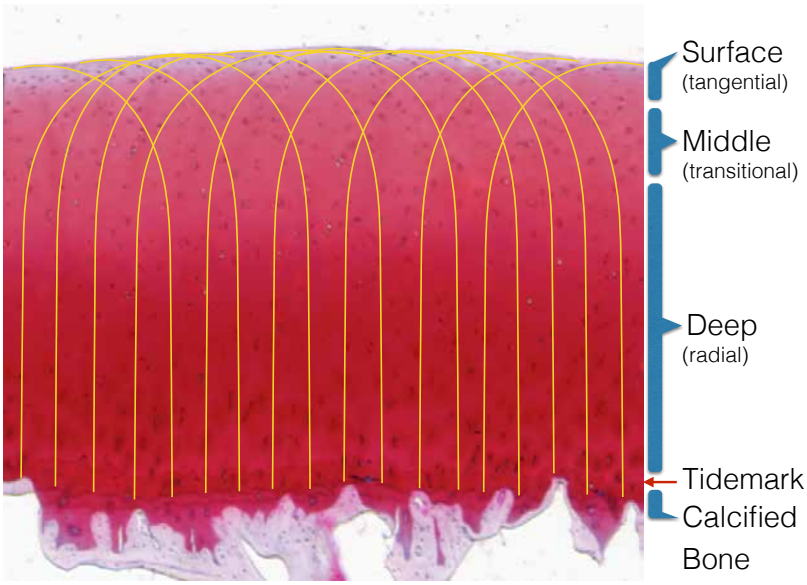

Figure 2.1: Structure of human articular cartilage. The red-coloured Safranin-O stain binds to negative charge (GAGs) in tissue and shows the PG distribution of cartilage. The PG concentration increases with tissue depth, but near to the calcified zone the PG content slightly decreases. In superficial and middle zones cells are single, while in the deep cartilage cells tend to group in vertical stacks of few chondrocytes. The cell size slightly increases whereas the cell density decreases towards the deep cartilage.

content. PG aggregates are larger and more saturated with aggrecan than in the middle or superficial layers. The collagen fibrils are large and form bundles, and the collagen content slightly increases towards the cartilage-calcified cartilage interface [43]. In the deep tissue chondrocytes display high variable shapes [38] and tend to be arranged in vertical stacks [41].

The interface between the deep zone and calcified cartilage is called the tidemark. Cartilage deformations terminate at the tidemark zone, which is also postulated to be different between areas subjected to axial and shear loading [44]. Calcified cartilage (3–8% of the thickness [45]) anchors the collagen fibrils and cartilage to the subchondral bone. Mechanical stiffness of calcified cartilage lies between those of cartilage and subchondral bone [46].

There are variations in the contents of the major components of articular cartilage *i.e.* collagen, PG, and water; these can be detected not only in different degrees of cartilage degeneration but also between species (Table 2.1). The organization of the collagen network varies with tissue depth and proximity to the chondrocytes. The organization of the collagen fibre bundles is suggested to be leaflike in structure [47–49]. The fibril diameter increases towards the deep cartilage, ranging from 25 nm up to 160 nm [50,51]. Different collagen types have distinctive roles in cartilage. The most abundant collagen types in adult human articular cartilage are type II (90%) and type III (10%) [52]. Collagen type II provides tension against swelling caused by water bound to PGs. Collagen type III is believed to modify the fibril network in response to matrix damage [53]. Other types of collagen are involved in fibril interactions with PGs, regulate the fibril size, organize the fibrils, or attach chondrocytes to the matrix [54].

The PG content of articular cartilage varies at different sites of the joint [61], but in general, its concentration increases with tissue depth [62]. PG aggregate (a form of aggrecan) consists of a hyaluronic acid backbone in which the core proteins are covalently bound. In addition, human PG aggrecan exhibits size polymorphism between individuals [34]. Chondroitin sulphate and keratan

Table 2.1: Composition of articular cartilage (% of wet weight). In arthritic cartilage, the water content tends to increase, and PG and collagen contents decrease.

Component	Human	Arthritic	Bovine	Reference
Water (%)	60–85	+3...+6	76–86	[35,55,56]
Collagens (%)	10–25	–1...–4	8–10	[35,55–57]
Proteoglycans (%)	4–10	–1...–5	2–14	[12,56,58]
Chondrocytes (%)	1–2	–0...–0.1	4–5	[41,59,60]

sulphate chains, *i.e.* glycosaminoglycan (GAG) chains, are bound to the core protein. The negative charge of PG is attributable to the presence of sulphate and carboxyl groups, and this represents the fixed charge density (FCD) of cartilage. For example, in bovine articular cartilage, the FCD increases from 90 to 400 nmol/mm^3 towards the cartilage bone interface [63]. PGs regulate tissue pore size, which has been estimated to range from 2 to 6 nm, and hydration [35]. PGs attract water and create the cartilage swelling pressure. The water content decreases with tissue depth from 80% in the superficial layer to 65% in the deep cartilage [64]. The water content of normal articular cartilage tends to decrease with age [65]. PGs have a variety of other functions including also modulating metabolism and maintaining the integrity of cartilage [34,66].

Articular cartilage is sparsely populated by chondrocytes, these cells occupy less than 2% of the total cartilage volume [41]. The cell diameter varies between 10 and 15 μm, slightly increasing towards the deep cartilage [67]. Instead, the cell density decreases from 24 000 to 8 000 1/mm^3 towards the deep cartilage [41,68]. In addition, the cell density decreases with age [69].

Articular cartilage responds to changes in the loading conditions. Thus, the maintenance of normal composition and structure requires joint loading and motion [70]. Furthermore, cellularity and the rate of matrix turnover vary in articular cartilage in different locations within the joint and also between joints [68].

2.2 MECHANICAL PROPERTIES

Articular cartilage has a mechanical function, and it possesses a unique weight bearing capacity. Not only does it distribute the joint loads and dampen the mechanical forces impacting on the joint, but it also lubricates the sliding surfaces and provides low friction for moving joints.

The ability of articular cartilage to function critically depends on the integrity of the collagen network and PG concentration. In conjunction with the intercollagen links and PG-collagen bonds, they account for the stiffness and strength of articular cartilage. The collagen network is mainly responsible for the dynamic response, while PGs contribute most to the static compressive properties of articular cartilage [71]. The swelling of PGs against the collagen framework and the mutual repulsion of negative charges effectively resists compressive loads [72,73]. The mechanical response is also strongly associated with the flow of fluid through the tissue. Under impact loads, there is no time for the fluid to flow relative to the solid matrix and no change in tissue volume occurs during loading [74].

Cartilage exhibits different mechanical properties during tension and compression [75] with the properties depending on the loading rate and magnitude [76,77]. When there is an abrupt load, articular cartilage behaves like an incompressible material (Poisson's ratio of 0.5). At mechanical equilibrium the Poisson's ratio of articular cartilage is reported to range from 0 to 0.4 [35,78], and to increase with depth in articular cartilage [79]. The tensile properties are primarily controlled by the collagens; the compressive properties are regulated by PGs and the water content [80]. If there is loading at slow rate, the collagen network alone is responsible for tensile strength and stiffness of cartilage. In contrast, at high rates of loading, it is the interaction between collagen and PGs which is responsible for the tensile behaviour. Tensile strength of articular cartilage of old people is lower than that of young individuals [81].

2.3 CARTILAGE DEGENERATION

In osteoarthritis, the cartilage matrix slowly degenerates. Many factors can contribute to degeneration of cartilage tissue, and eventually to (secondary) osteoarthritis *e.g.* excessive impacts, joint-stressing sports, abnormal joint loading, obesity or simply aging. Especially the way in which the activity is performed, *i.e.* the loading rate rather than magnitude, may determine the development of matrix damage [82]. Uninterrupted pressure may also lead to severe damage in cartilage [83, 84]. In addition, genetic factors are known to be strong determinants of OA [85].

Articular cartilage has a very limited capacity to repair itself after a mechanical injury [86]. Since cartilage lacks blood vessels, it does not respond to injury with inflammation. An injury may jeopardize also the well-being of adjacent cartilage and can result in OA.

Structure and composition of degenerated articular cartilage

The early signs of degeneration of articular cartilage include surface fibrillation, PG loss and an increase in the water content [9]. Molecular fragments may be found in the synovial fluid [87], and the cartilage may thicken and appear more opaque [40]. The collagen network degrades at the surface and there are reductions in both the amounts and size of the PGs [35,88]. However, the PG concentration may increase deeper in the cartilage. Chondrocytes can respond to mechanical stimulation and thus changes in the mechanical environment of chondrocytes affect cartilage metabolism [35].

Later signs of cartilage degeneration are erosion of articular surface, fissures, ulceration and thinning [24]. The PG molecules appear to be larger than in healthy cartilage [35,89]. Chondrocyte size in the superficial and middle layers increases with cartilage degeneration. In addition, late stage osteoarthritis is linked to increased formation of cell clusters [90, 91]. Calcification of the meniscus has been speculated to be a factor contributing to OA [92, 93], although knee condylar cartilage calcification is considered to be linked more

to aging than OA [94].

It has been shown that immobilization of the joint causes both a thinning and a decrease in the PG content of articular cartilage. On the other hand, moderate physical exercise can increase both the PG concentration and thickness of articular cartilage [14,95].

Mechanical properties of degenerated cartilage

Changes in the structure and composition sensitively affect the mechanical behaviour of the tissue. The roughening of the articular surface alters fluid transport properties across the surface [35]. Since the water content increases, this causes the compressive and tensile stiffness to decline and the cartilage's permeability increases [9,35] *i.e.* cartilage appears to soften. Together, these changes result in a more extensive and a faster deformation of OA cartilage under loading.

2.4 DIAGNOSTICS OF CARTILAGE DEGENERATION

The development of OA may be asymptomatic and it can take years until a cartilage injury can be detected through changes in bone or other structures surrounding the joint. A clinically relevant degeneration in articular cartilage is one that alters joint function or causes pain [20]. Unfortunately, at this stage, the progression of OA may be irreversible.

The clinical diagnosis of osteoarthritis is based on symptoms described by the patient; manual clinical examinations on joint motion, position and appearance; radiological findings; and differential laboratory diagnosis. A precise diagnosis enables accurate treatment [20]. The initial degenerative signs in cartilage may remain undetected due to a lack of tissue loss and marginal superficial changes. The symptoms of advanced OA may involve joint pain or stiffness and a limited ability to function. Joint mobility can be reduced, or the joint may lock because of loose fragments of cartilage or meniscus.

The most common imaging modalities applied in OA diagnostics include radiography, magnetic resonance imaging (MRI), ultrasound imaging and arthroscopic examination (Table 2.2).

Radiography
Radiography is the standard procedure used for OA diagnosis. It is a simple and low cost imaging technique [97], and it can also be used to determine the progression of the disease [20]. The Kellgren-Lawrence OA grading scale was introduced in the 1950s and is still widely used [96,102]. However, radiography reveals only the joint space width, and osteoarthritic changes in bone (subchondral sclerosis, cysts, osteophytes). At this stage, the articular cartilage has become injured in an irreversible manner and is significantly thinner.

Radiography is a 2D imaging modality exposing patient to a minimal radiation dose. The dose from a knee radiography is equivalent to the background radiation dose of one day, while X-ray tomography of a knee is equivalent to a background radiation dose of 60 days [103,104]. However, modern CT devices may reduce the dose to being equivalent to a few days of background exposure [7]. The average background radiation dose is 3.2 mSv per year in Finland [105].

Arthroscopy
The integrity of the articular surface may be visually evaluated in arthroscopy. Arthroscopy is a standard technique in the evaluation of cartilage lesions, although it should only be performed for therapeutic reasons [98]. Arthroscopy can be combined with mechanical indentation, which provides information on OA related superficial degeneration of articular cartilage [106].

External ultrasound imaging
Invasive ultrasound imaging performed during an arthroscopic examination can provide information about variations in cartilage thickness, surface roughness, and even signs of degeneration of the

Table 2.2: Advantages and challenges of clinical methods which can be used in the diagnostics of cartilage degeneration.

Method	**Advantages**	**Challenges**	**Reference**
Clinical examination	Good availability, easy to perform	Subjective, limited sensitivity	[18]
X-ray radiography	Good availability, easy to perform, simultaneous imaging of subchondral bone, standardized method	Poor soft tissue contrast, poor sensitivity	[96,97]
Arthroscopy	Visualized articular surfaces, medical interventions simultaneously possible	Invasive, subjective	[98]
External ultrasound examination	Good availability, fast (10 min)	Limited resolution, restricted reach	[99]
MRI	Soft tissue contrast	Imaging time (30–60 min), limited availability (costs)	[100]
dGEMRIC	Sensitivity to composition	Limited resolution, possibly harmful contrast agent	[101]
CECT	Good availability, fast scanning time (1 min), sensitivity to composition, relatively good resolution	Radiation dose, possibly harmful contrast agent	[6]

collagen network [107, 108]. Instead, external ultrasound findings may detect cartilage degeneration, but unfortunately the failure to observe these signs cannot exclude the possibility of cartilage degeneration [99]. It has been claimed that ultrasound may be more useful in a survey of the joint effusion and inflammation than in the examination of cartilage [109].

Magnetic resonance imaging

Magnetic resonance imaging (MRI) is a technique that can highlight different tissue types by manipulation of contrast via the appropriate choice of imaging parameters [110]. Its strength is in its good soft tissue contrast, which enables quantitative measurements of cartilage volume and thickness. MRI can detect several characteristic features of OA. For example, the T2 relaxation time of articular cartilage is sensitive to the collagen concentration and architecture [111], and diffusion effects may be detectable with appropriate MRI pulse sequences [112].

In delayed gadolinium enhanced magnetic resonance imaging of cartilage (dGEMRIC), the paramagnetic contrast agent gadopentetate is transported into cartilage. In this method, the mobile anionic contrast agent molecules distribute into the cartilage in inverse proportion to the amount of GAGs [3]. An increase in the gadopentetate concentration is reflected as a decrease in the T1 relaxation time. In the clinical dGEMRIC protocol, the joint is exercised for 10 minutes after contrast agent injection and imaged 1-2 hours after injection [113–115]. MRI has been used *in vivo* to reveal cartilage deformation after exercise, and dGEMRIC has been able to demonstrate recovery after cartilage repair surgery as well as the relationship between exercise and GAG content in human knee cartilage [116–118].

3 Diffusion in articular cartilage

Diffusion refers to the transfer of a substance through a medium due to random molecular motions [119]. The basis for diffusion is that there is a concentration gradient down which the substance travels [120]. In living material, there are always processes that generate these kinds of gradients. In general, the rate of diffusion depends on several factors, *i.e.* the concentration differences, pressure, temperature and composition [120, 121]. However, diffusion is a slow process. Typically the diffusion rate is around cm/min in gases, less than mm/min in liquids, and μm–nm/min in solids [122, 123].

In physics and biology, diffusion is commonly described with Fick's laws which makes it possible to derive the diffusion coefficient. Instead, in chemical kinetics and medicine, a mass transfer coefficient is typically calculated [123]. In this study, the diffusion coefficient approach was selected.

3.1 DIFFUSION THEORY

The mathematical theory of diffusion is based on the hypothesis that the rate of transfer of a diffusing substance is proportional to its concentration gradient [119]. The diffusion coefficient D is a measure of the rate at which molecules pass down a concentration gradient. It represents the amount of material that in a unit time and with a unit concentration gradient would cross a plane of unit area normal to the direction of diffusion. D can be measured by observing the rate at which a boundary spreads or the rate at which a more concentrated solution diffuses into a less concentrated one [124].

Fick's first law

In Fick's law (Eq. 3.1) the concentration C is related to diffusive flux J via the diffusion coefficient D, and the area A through which the diffusion occurs. In one dimension Fick's law is

$$J = -AD\frac{\partial C}{\partial x}, \tag{3.1}$$

where the minus sign indicates that the net flow of diffusing material is towards a decreasing concentration. This law does not take into account convection, which in dilute solutions is negligible [123]. As a consequence, one should be cautious when using Fick's law at very high concentrations, or when a concentration change occurs abruptly. However, this law can usually be employed in solving practical problems related to diffusion in biological materials [120].

One dimensional diffusion can be readily approximated with the Fourier number Fo (Eq. 3.2), where L has the dimension of length [121,123].

$$Fo = \frac{Dt}{L^2} \tag{3.2}$$

The Fourier number is dimensionless and is used to approximate unsteady-state mass transfer.

Fick's second law

In Fick's second law, the rate of change of concentration is proportional to the rate of change of the concentration gradient. For a constant diffusion coefficient, it is

$$\frac{\partial C}{\partial t} = D\frac{\partial^2 C}{\partial x^2}. \tag{3.3}$$

However, the diffusion coefficient may not be constant. A concentration dependence exists in many systems, but in dilute systems, its dependence is small, and D can be assumed to be constant for practical purposes [119]. When including concentration depen-

dence, the Fick's second law takes the following form (Eq. 3.4):

$$\frac{\partial C}{\partial t} = \frac{\partial}{\partial x}\left(D(C)\frac{\partial C}{\partial x}\right). \tag{3.4}$$

Nernst equation

The relative amounts of reactants and products in a chemical reaction (Eq. 3.5)

$$\alpha A + \beta B \rightleftharpoons \sigma S + \tau T \tag{3.5}$$

are described with the reaction quotient Q_r (Eq. 3.6)

$$Q_r = \frac{\{S_t\}^{\sigma}\{T_t\}^{\tau}}{\{A_t\}^{\alpha}\{B_t\}^{\beta}}, \tag{3.6}$$

where $\{X_t\}$ is the instantaneous activity of an ion X at time t. In general

$$Q_r = \frac{\prod_j a_{j(t)}^{\nu_j}}{\prod_i a_{i(t)}^{\nu_i}}, \tag{3.7}$$

where reaction product activities a_j and reactant activities a_i are raised to a power of the corresponding stoichiometric coefficients ν_j and ν_i. At equilibrium ($t = \infty$), the reaction quotient becomes a constant. In practical calculations, and with dilute solutions, chemical activities are typically approximated by concentrations.

The Nernst equation (Eq. 3.8) relates the concentrations to electrical potential. At equilibrium

$$E = \frac{RT}{zF}\mathrm{Ln}(Q_r), \tag{3.8}$$

where R is the molar gas constant, T is the absolute temperature, F is the Faraday constant, and z is the number of moles of electrons transferred.

Donnan equilibrium

Donnan equilibrium theory (Eq. 3.9 and 3.10) defines a simple but well applicable relationship for ions in equilibrium [125, 126]. This

theory depends on assumptions that there is the existence of an equilibrium, and that there is a constraint which restricts free diffusion of one (or more) electrically charged constituent. The constraint in articular cartilage is FCD.

$$\frac{RT}{zF}\mathrm{Ln}\left(\frac{[S]^{\sigma}[T]^{\tau}}{[A]^{\alpha}[B]^{\beta}}\right)=0 \tag{3.9}$$

$$\frac{[S]^{\sigma}}{[A]^{\alpha}}=\frac{[B]^{\beta}}{[T]^{\tau}} \tag{3.10}$$

Using logarithm rules in Eq. 3.9 the desired concentration relationship (*e.g.* Eq. 3.10) can be calculated.

3.2 SOLUTE DIFFUSION IN ARTICULAR CARTILAGE

Articular cartilage is a porous, biphasic composite material, which consists of layers with different structure, composition and diffusion properties. The chondrocytes are totally dependent on the diffusion of nutrients in articular cartilage, *i.e.* small solutes like oxygen and glucose are transported mainly by diffusion [127,128]. The diffusion of nutrients has been reported to regulate the chondrocyte density and an impaired nutrient supply reduces the number of viable chondrocytes [129–131].

Diffusion is faster at higher temperatures because of higher kinetic energy of molecules, *i.e.* quicker Brownian motion. However, in the human body, the variation of temperature is very minor, only in the range of few degrees [132].

In general, the compression of a material decreases the free mean path of a molecule, which leads to a decreased diffusion coefficient. Compression decreases cartilage permeability, solute diffusivity, and partition coefficient of a substance [78, 133]. Theoretically, if articular cartilage is subjected to a major strain, then the diffusion of a large solute would favor movement in a direction perpendicular to compression [134].

The diffusion rate is dependent on the medium in which it is

taking place, being fastest in gases and slowest in solids. In solids, the path a molecule has to take is tortuous, making diffusion very slow. Correspondingly, increases in the solid content of articular cartilage, *i.e.* collagens and PGs, diminish diffusion [134–142]. Furthermore, collagen network organization and collagen fiber orientation may affect diffusion [143].

The matrix pore size and its structure as well as pore connectivity affect solute diffusion in cartilage [144]. Diffusion is hindered when solute size approaches the pore size, which in deep cartilage is only a few nanometers [145]. Thus, the diffusion of large molecules depends strongly on the pore size distribution within the cartilage [146].

Typically in cartilage, permeability increases in conjunction with the water content, *i.e.* permeability is highest below the superficial layer and decreases towards the articular surface and middle zone being lowest in the deep cartilage [144, 147]. In intact human knee articular cartilage, the mean permeability has been estimated to be 25×10^{-15} $\mathrm{m}^4/\mathrm{N\,s}$ normal to articular surface, and half of that value in a direction parallel to the articular surface [78].

The diffusion coefficient is inversely proportional to the radius of a particle, or to the square root of molecular mass, or the cube root of particle volume. In addition, hydration may change the effective radii of the diffusing molecule, which in turn will affect its rate of diffusion [120, 148, 149].

Cartilage possess an intrinsic negative fixed charge density (FCD) arising from the presence of anionic PGs. Thus anionic molecules are confronted by a repulsive force, whereas cationic molecules of the same size can pass more quickly through the cartilage matrix [36]. Thus, a change in the FCD may modify the diffusion of a charged molecule.

The effect of solute concentration on the diffusion properties in articular cartilage is controversial [150, 151]. In a biological environment, the concentration dependence of the diffusion coefficient may emerge only with highly concentrated solutes [119].

Table 3.1: The factors affecting solute diffusion in cartilage.

Diffusion increases	**Feature in cartilage**
Temperature ↗	Body temperature, joint inflammation
Porosity ↗	Cracks in cartilage matrix
Pressure ↘	Joint movements, cartilage compression
Tortuosity ↘	Fiber linking, solid content
Molecule size ↘	Hydrodynamic radius
Matrix viscosity ↘	ECM stiffening with increasing substances

4 Contrast enhanced computed tomography of cartilage

The X-ray attenuation in a substance depends on the characteristics of the material in question and the energy of X-rays. Bone is a relatively dense material and it consists of atoms with a relatively high proton number ($^{31}_{15}P$, $^{40}_{20}Ca$) causing elevated X-ray absorption, leading to good contrast in traditional X-ray images. In contrast, soft tissues may be difficult to visualize, especially the discrimination of normal tissue from pathological tissue may be challenging due to their minor differences in X-ray attenuation. X-ray tomography provides 3D characterization and improved contrast over traditional X-ray images. However, soft tissue contrast is still somewhat limited also in tomographic images.

4.1 CONTRAST AGENTS

The X-ray opacity of tissue can be improved by administration of a contrast agent. Heavy atoms can be attached to functional molecules targeting specific structures. In CECT, X-ray attenuation is increased by injecting a contrast agent, typically containing either iodine or gadolinium.

The contrast agent can be administered intravenously as in dGEMRIC [113], or intra-articularly as in the CECT of articular cartilage of the knee [6, 7]. Intravenously administered contrast agent will be diluted as soon as it gains access to the vascular system and will be rapidly distributed throughout the body. Instead, in intra-articular injection, the contrast agent is administered directly into the joint capsule. The contrast agents used in this study are mainly excreted within a few hours after administration and typically nearly all of contrast agent will have been eliminated from

the body within 24 hours [152–155]. There are patient safety issues to be considered with this procedure since it must be remembered that contrast agents may have biological interactions and there may be individuals who are particularly sensitive to the toxic effects of these compounds [156–158].

4.2 BASIC PRINCIPLES OF CECT

Differences in tissue structure and composition will be reflected in differences in the accumulation of the contrast agent inside the tissue. In articular cartilage, the intrinsic negative fixed charges of PGs create an environment in which charged mobile molecules diffuse to reach Gibbs-Donnan equilibrium [144]. In addition to the fixed charge, solid cartilage matrix formed by PGs and collagen hinder diffusion of mobile molecules. As a result, the diffusion of the charged contrast agent molecules reflect the composition of the cartilage.

The uptake of anionic contrast agent is hypothesized to be inversely proportional to the PG distribution in cartilage [4]. In contrast, cations are assumed to diffuse into the cartilage proportionally to the fixed charge density (FCD) [159]. An electrically neutral solute is postulated to diffuse into cartilage in inverse proportion to the solid content. In both situations, it is assumed that mobile molecules have sufficient space to allow them to move through the medium.

The amount and distribution of proteoglycans and hence the tissue fixed charge density are known to change in OA. The reduction of negatively charged PGs in degenerated cartilage decreases the repulsion forces on the negative contrast agent molecules and the contrast agent will be able to penetrated better into the cartilage [33]. A breakage of the collagen network results in an increase in the water content through PG attraction to water and again the contrast agent molecules will have more space in which to diffuse in articular cartilage. In addition, other pathological signs such as surface fibrillation and fissures increase the diffusion rate of the

contrast agent into the tissue [2]. In addition to the evaluation of cartilage composition, the use of a contrast agent enhances the image contrast thus improving the visualization of features of the cartilage morphology, such as tissue thickness and lesions [5].

Multiple names have been bestowed on the method of contrast enhanced imaging of cartilage with X-rays. For example, in the Guldberg Musculoskeletal Research Laboratory, a microCT technique that relies on equilibrium partitioning of an ionic contrast agent (EPIC-μCT) is used [5]. A delayed computed tomography arthrography, delayed quantitative computed tomography (dQCT) arthrography, and delayed cone beam computed tomography (delayed CBCT) arthrography terms are also used [6,7,115]. In many situations, the method is called contrast enhanced CT, or contrast enhanced computed tomography (CECT). In all of these techniques, the principle is the same *i.e.* charged contrast agent is applied and CT is used to visualize cartilage morphology or contrast agent penetration into articular cartilage.

5 Aims of the present study

The focus of this study was to investigate the interrelationships between cartilage matrix, the properties of contrast agent and the diffusion and distribution of contrast agent within a tissue.

The specific aims of this study were

1. To characterize the feasibility of utilizing CECT to detect spontaneous degeneration of articular cartilage.
2. To determine the diffusion rate and equilibrium distribution of an anionic contrast agent in human articular cartilage.
3. To investigate the effect of molecule size and charge on the diffusion of MR and CT contrast agent into articular cartilage.
4. To study the effect of contrast agent concentration on its diffusion into articular cartilage.

6 Materials and methods

This thesis work consists of four independent studies I-IV. The materials and methods used are summarized in Table 6.1. Samples from the knees used in study II were gathered for an earlier study with permission from the National Supervisory Authority for Welfare and Health (TEO 1781/32/200/01) [160]. Bovine knees were obtained from a local abattoir (Atria Oyj, Kuopio, Finland).

6.1 ARTICULAR CARTILAGE SAMPLES

In studies I and II, osteochondral cylinders were investigated. The CECT measurements were conducted on samples stored in a freezer and thawed just prior to the experiment. In studies III and IV, cartilage discs were investigated. The cartilage discs were prepared from patellae within a few hours post-mortem. During preparation, the samples were kept moist with intermittent spraying with phosphate buffered saline (PBS). The CECT measurements were started shortly after specimen preparation.

6.2 CONTRAST AGENT TREATMENT OF THE SAMPLES

In the present study, four different contrast agents were used: Sodium iodide, ioxaglate, gadopentetate and gadodiamide (Table 6.2). Sodium iodide is a small molecule that dissociates into its atomic size components, *i.e.* cationic sodium and anionic iodide. The anionic ioxaglate molecule contains six iodine atoms ($^{127}_{53}I$) [153], and gadopentetate and gadodiamide molecules both contain one gadolinium atom ($^{158}_{64}Gd$). The K-edge is 33 keV for iodine, and 50 keV for gadolinium [161].

All studies were conducted at room temperature. In all studies, the contrast agent treatment was carried out with inhibitors of proteolytic enzymes to prevent cartilage decomposition during

Table 6.1: Summary of materials and methods used in studies I–IV.

Study	Samples	*n*	Diameter	Methods and Parameters
I	Bovine osteochondral cylinders	3	18 mm	CECT (partition over 27h)
	Bovine osteochondral cylinders	32	18 mm	CECT (partition at 24h) Histology (Mankin score†) Quantitative microscopy (GAG content†: Safranin-O staining and uronic acid content) Mechanical (Young's modulus†, Cartilage thickness)
II	Human TMP Human FMC (Osteochondral cylinders)	12 12	4.0 mm 4.0 mm	CECT (partition over 24h) Histology (Mankin score†) Quantitative microscopy (GAG distribution†: Safranin-O staining and uronic acid content) Biochemistry (Water content†) Cartilage thickness†
III	Bovine cartilage discs	64	4.0 mm	CECT (partition over 29h and 35h wash out, *n*=24: partition over 5 days) Optical microscopy (Cartilage thickness) Biochemistry (Water content)
IV	Bovine cartilage discs	96	4.0 mm	CECT (partition over 29h, Diffusion coefficient: FE-model) Optical microscopy (Cartilage thickness) Quantitative microscopy (GAG distribution: Safranin-O staining) Biochemistry (PG content, Water content, Collagen content)

n = number of samples, CECT = contrast enhanced computed tomography (and diffusion time), PG = proteoglycan, FMC = femoral medial condyle, TMP = tibial medial plateau, FE = finite element. † = extracted from our earlier study.

the measurements. The inhibitors were ethylenediaminetetra-acetic acid disodium salt (EDTA) and benzamidine hydrochloride hydrate. In study III, the concentrations of different contrast agent species were chosen to provide similar signal-to-noise ratios. Each solution was adjusted to have isotonic osmolarity ($\sim$ 300 mOsm) with tissue plasma and a physiological pH value of 7.4.

Table 6.2: Contrast agents (charge of the molecule) used in studies I–IV. Direction of diffusion and time points of imaging are also shown.

Study	Contrast agent	c (mM)	M (g/mol)	Diffusion, Time points
I	Ioxaglate (-1)	21	1269	Through all sample surfaces 2, 4, 6, 8, 23, 25, 27 h
	Ioxaglate (-1)	21	1269	24 h
II	Ioxaglate (-1)	21	1269	Through all sample surfaces 2, 4, 6, 8, 10, 12, 14, 16, 18, 20, 22, 24 h
III	Ioxaglate (-1) Iodide (-1) Gadopentetate (-2) Gadodiamide (0)	21 134 100 180	1269 127 548 574	Either through articular surface or deep cartilage IN: 1, 5, 9, 16, 25, 29 h and 2 d, 3 d, 4 d, 5 d OUT: 1, 5, 9, 16, 25, 29, 35 h
IV	Ioxaglate (-1)	5, 10 21, 50	1269	Through articular surface
	Iodide (-1)	30, 60 126, 300	127	1, 5, 9, 16, 25, 29 h

c = contrast agent bath concentration, M = molar mass.

6.3 CECT MEASUREMENTS AND ANALYSES

A clinical pQCT device (XCT 2000, StraTec Medizintechnik GmbH, Pfortzheim, Germany) was used for all CECT measurements. The

slice thickness was 2.3 mm, and the in-plane pixel size was 0.20×0.20 mm^2. The X-ray tube voltage was 58 kVp, and 360 imaging projections were applied. Five overlapping cross-sections were averaged to reduce the background noise. Contrast agents and diffusion geometries are summarized in Table 6.2.

In all studies, the attenuation map of native cartilage was recorded just before immersion in contrast agent. The attenuation maps were converted into attenuation profiles and the profile of native cartilage was subtracted from the contrast enhanced attenuation profile. In study III, the attenuation maps were subtracted. The attenuation profile was then determined and transformed to provide the contrast agent concentration profile. To achieve this transformation, the attenuation was linearly converted into the contrast agent concentration, defined as moles of solute per volume of tissue. X-ray absorption was calibrated with series of known contrast agent concentrations in order to achieve a quantitative determination of the contrast agent concentration in cartilage.

Partition coefficients were calculated from the concentrations of the contrast agent with equation 6.1.

$$\frac{c_{cartilage}}{c_{bath}} \times 100\% \tag{6.1}$$

The diffusion coefficient in study IV was calculated using a one dimensional finite element model based on the Fick's second law.

6.4 REFERENCE METHODS

In studies I and II, all reference parameters were obtained from previous publications from our laboratory [58, 160]. CECT parameters were compared to the Mankin score (studies I and II), to the uronic acid content (studies I and II), to the GAG concentration profile (study II), the water content (studies II and IV), as well as to Young's modulus (study I).

Cartilage adjacent to CECT imaging was used in the chemical analyses of tissue composition (studies I-IV). The water content was

determined as difference between the wet and dry weights. The wet weight of the cartilage was measured after PBS immersion and the dry weight after freeze-drying.

The uronic acid (studies I and IV) and hydroxyproline (study IV) contents were quantified spectrophotometrically [162, 163], and normalized to wet weights to compensate for variations in sample sizes. The uronic acid content is linearly related to PG content, whereas the hydroxyproline content reflects the collagen content [162, 164, 165].

The PG distribution was determined from Safranin-O stained histological sections by measuring the optical density of stained histological samples (studies II and IV). Safranin-O binds stoichiometrically to the negative charge in cartilage which corresponds to the PG content.

The Mankin score (studies I and II) was determined by calculating the average of three independent evaluations of cartilage histological integrity in the Safranin-O stained sections. The Mankin score is a sum of grades for cartilage structure abnormalities, cell distribution and density, Safranin-O stain distribution, and tidemark integrity. The higher the score (range from 0 to 14), the more abnormalities that are present in the cartilage [166].

Young's modulus was determined using stepwise stress-relaxation measurements in unconfined compression geometry (study I). The cartilage thickness was determined as the pre-stress distance between the compressive plates of the material testing device (study I), from CECT images (studies I and II), as well as with optical microscopy (studies III and IV).

6.5 STATISTICAL ANALYSES

In study I, Mann-Whitney U test was used to test the significance of differences between the normal and spontaneously degenerated sample groups. Spearman correlation analysis was used to relate Mankin scores with other parameters, and Pearson correlation analysis was applied for other correlation analyses.

In study II, Wilcoxon signed ranks test was used to investigate statistical significance of differences in parameters of different sample groups. Spearman correlation analysis was used to relate Mankin scores with other parameters. Pearson correlation analysis was applied to relate CECT results to water and uronic acid contents.

In study III, Wilcoxon signed ranks test for two related samples was used to investigate statistical significance of differences in diffusion through the articular surface and deep cartilage.

In study IV, the exact Wilcoxon signed ranks test for two related samples was applied to investigate statistical significance of differences in contrast agent partition coefficients, partitioning profiles, and diffusion coefficients between the different contrast agent bath concentrations. The exact Kruskall-Wallis test was used to test for differences in contrast agent partition and diffusion coefficients and in reference parameters between the sample groups.

Image analysis and calculations were conducted with Matlab (MathWorks Inc., Natick, MA, USA). In study II, the correlation between X-ray attenuation profiles of native cartilage and cartilage after 24 h immersion in contrast agent was calculated with Matlab. Other statistical analyses were conducted using SPSS software (SPSS Inc., Chicago, IL, USA).

7 Results

The results from studies I–IV are summarized in this chapter. A more detailed review of the results can be found in the original articles I–IV.

7.1 CONTRAST AGENT DIFFUSION AND DISTRIBUTION IN NORMAL AND DEGENERATED ARTICULAR CARTILAGE

In native cartilage, the X-ray attenuation increased along the tissue depth (Figure 7.1). In addition, the attenuation profiles of human cartilage before contrast agent immersion and after 24 hours of immersion in contrast agent were significantly ($p < 0.05$) inversely correlated ($r = –0.76 \pm 0.34$, $n = 24$, mean $\pm$ SD) (study II).

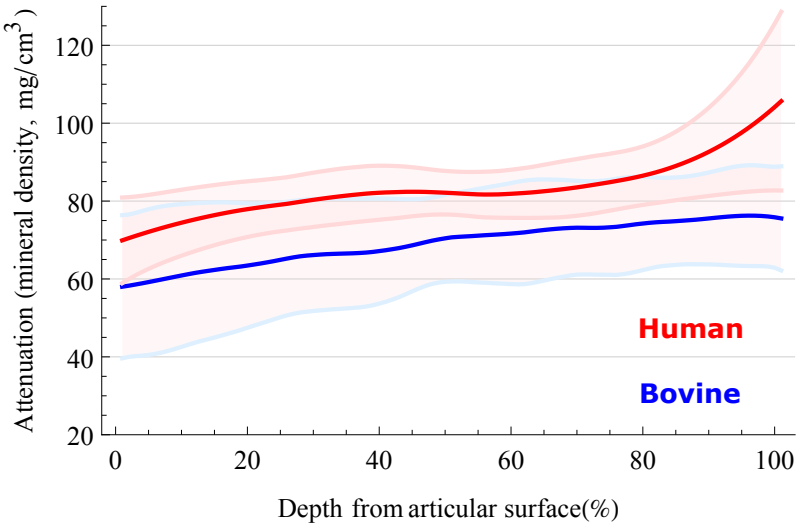

Figure 7.1: X-ray attenuation profiles of native articular cartilage (0 = articular surface, 100 = cartilage-bone interface). The shaded areas indicate standard deviations. Attenuation is expressed as calcium hydroxyapatite -equivalent bone mineral density (mg/cm^3).

The concentration of anionic ioxaglate was significantly higher (11%, $p < 0.05$) in the superficial layer of spontaneously degener-

ated cartilage than that of normal cartilage after immersion for 24 hours (study I, Figure 7.2). The correlations between the superficial contrast agent concentration and full thickness PG content (–0.64, $p < 0.01$, $n = 32$) or the Mankin score (0.46, $p < 0.01$) were stronger than those between full thickness contrast agent concentration and full thickness PG content (–0.53, $p < 0.01$) or Mankin score (0.25).

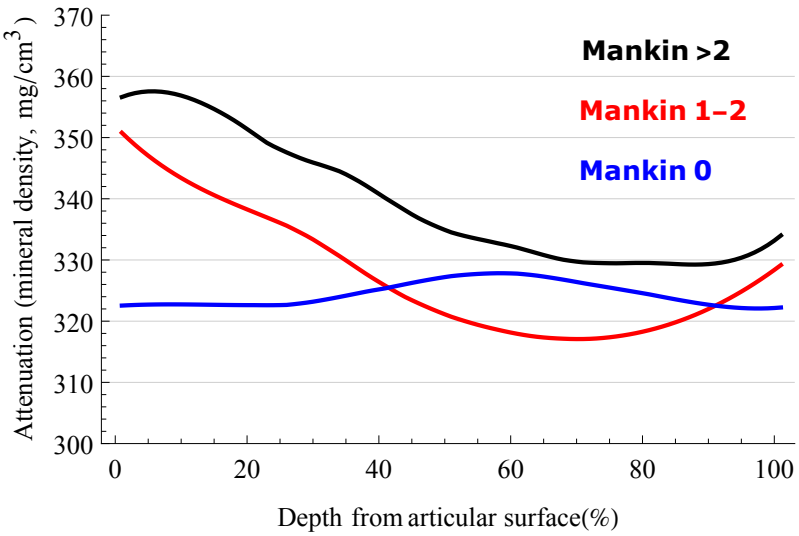

Figure 7.2: Contrast agent diffusion (ioxaglate 24h) distributions of intact and degenerated bovine articular cartilage (0 = articular surface, 100 = cartilage-bone interface). Attenuation is expressed in calcium hydroxyapatite -equivalent bone mineral density (mg/cm^3).

The diffusion of contrast agent through deep cartilage was slower than through the articular surface (study III). In addition, no evidence could be detected for contrast agent diffusion through subchondral bone (study II). The partitions of the contrast agent were lower in samples with diffusion through deep cartilage than in samples with diffusion through articular surface (study III). This was the case during the whole course of the diffusion experiments with ioxaglate, gadopentetate, and gadodiamide. With iodide, the difference in contrast agent partition between the diffusion directions disappeared after 16 hours.

In study I, the diffusion of the anionic contrast agent ioxaglate

took more than 8 hours to reach equilibrium. In studies II–IV, the diffusion of ioxaglate typically required at least 12 hours to reach near equilibrium and the diffusion was seen to continue as long as 24 hours. Only in thin (thickness = 0.8 mm) cartilage, was it possible to attain a situation of near equilibrium in four hours (study II).

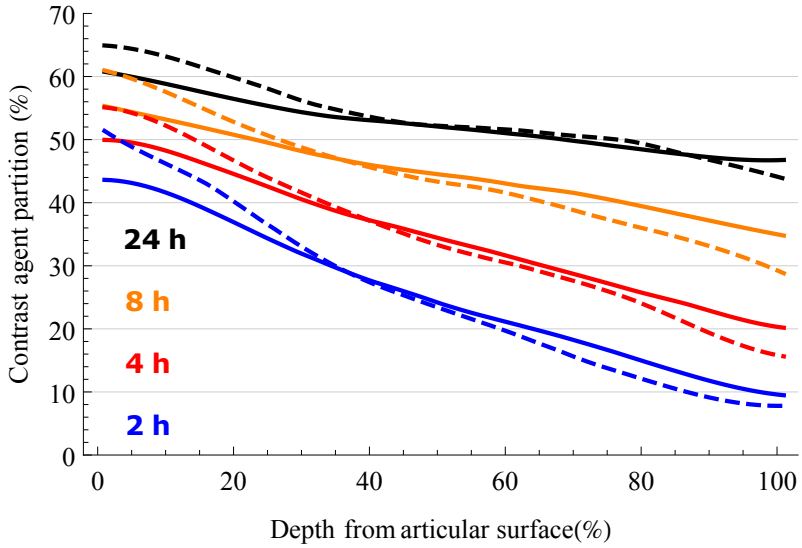

Figure 7.3: Contrast agent (ioxaglate) diffusion distributions in human FMC (solid lines) and TMP (dashed lines) articular cartilage. Contrast agent partition = $c/c_{bath} \times 100\%$. The horizontal axis shows the relative depth from the articular surface.

The contrast agent partition profiles were rather similar in human femoral (FMC) and tibial (TMP) articular cartilage (study II, Figure 7.3). However, more of the contrast agent gained access into the superficial TMP cartilage. Furthermore, slightly less contrast agent penetrated into the deep TMP cartilage. With human samples, the PG content profiles and the X-ray attenuation profiles correlated negatively (r = –0.83 $\pm$ 0.19, mean $\pm$ SD) already after 2 hours' immersion in the contrast agent, and the correlation remained almost constant for the remaining immersion time. The concentration of the bulk contrast agent correlated significantly with the uronic acid concentration (r = –0.76, p = 0.004) in FMC samples as well as with the Mankin score (r = 0.75, p = 0.005) in

TMP samples after 2 hours of immersion.

7.2 EFFECT OF CONTRAST AGENT PROPERTIES ON DIFFUSION AND DISTRIBUTION

The small size iodide diffused faster than the larger ioxaglate, gadopentetate or gadodiamide molecules (Table 6.2, Figure 7.4). It took over 12 hours for the larger molecules to reach near equilibrium. Instead, iodide reached near equilibrium in just a few hours. However, the diffusion of iodide through deep cartilage did not achieve the (near) equilibrium until 16 hours (study III).

The concentration profiles of all contrast agents at all timepoints displayed a downward slope towards deep cartilage when diffusive flux was through the articular surface. However, after the initial stages of diffusion through the articular surface, the contrast agent partition of the electrically neutral gadodiamide was seen to rise rather evenly until the 5 hour time point throughout the cartilage thickness, and later it increased more slowly in the surface region than in the middle and deep cartilage (study III). Instead, the distributions of anionic contrast agents showed slightly different behaviours (Figure 7.4). With respect to diffusion through the deep cartilage, the slopes of partition profiles were reversed.

At near equilibrium, the concentration profiles of the electrically neutral gadodiamide and the negatively charged iodide showed close to flat profiles when the diffusive flux was through the deep cartilage. In contrast, ioxaglate (q = –1) and gadopentetate (q = –2) displayed an upward slope towards deep cartilage even after 29 hours' diffusive flux through the deep cartilage. At near equilibrium, iodide (q = –1) reached similar distributions regardless of the direction of the diffusive flux.

The diffusive flux out from the articular cartilage was slower through the deep cartilage than through the articular surface (Figure 7.5). After 25 hours of diffusion, a small amount of contrast agent was still found in cartilage, with the exception of iodide.

There were no statistically significant differences in diffusion or

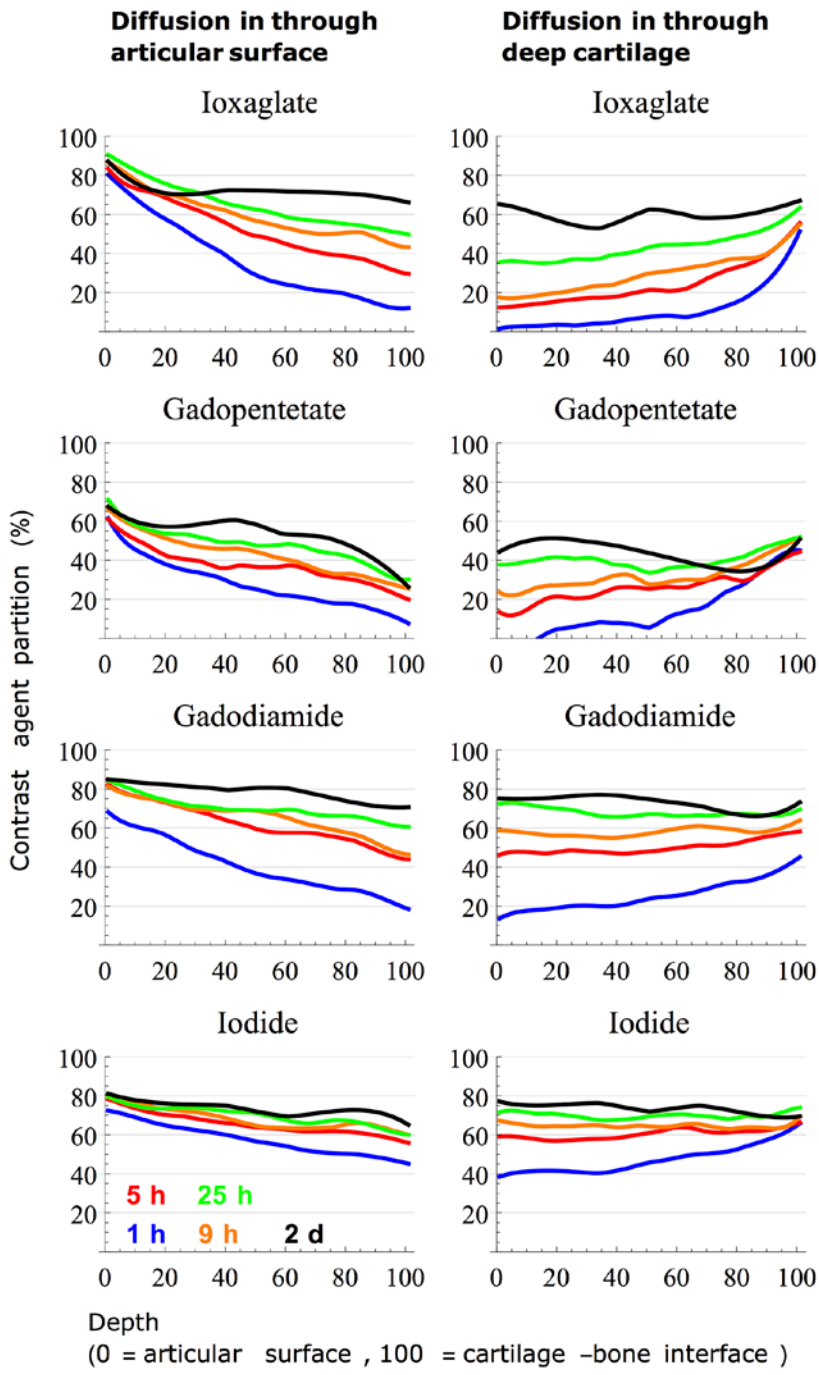

Figure 7.4: Contrast agent diffusion into bovine articular cartilage.

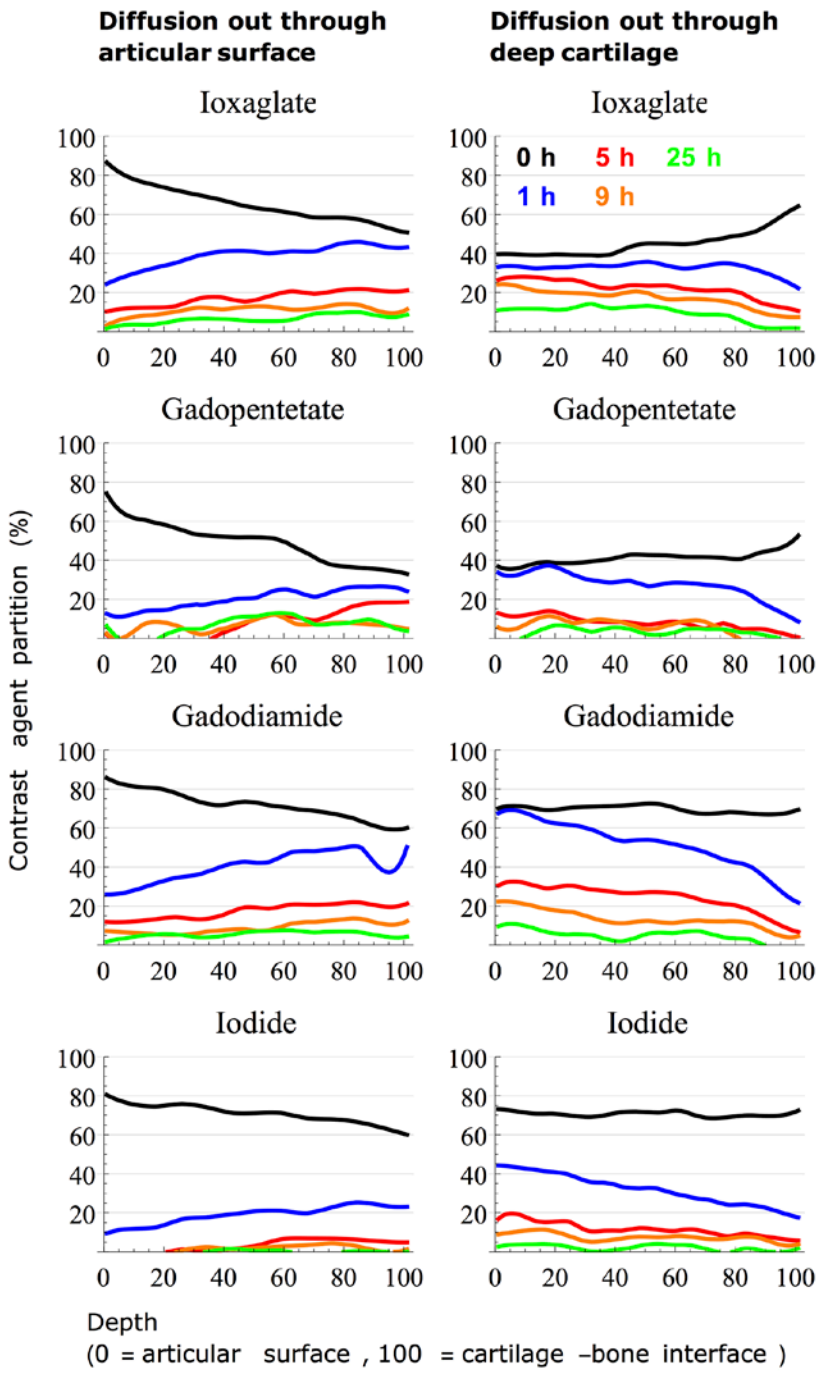

Figure 7.5: Contrast agent diffusion out from bovine articular cartilage. Black lines show near equilibrium distributions after 29 hours' diffusion in.

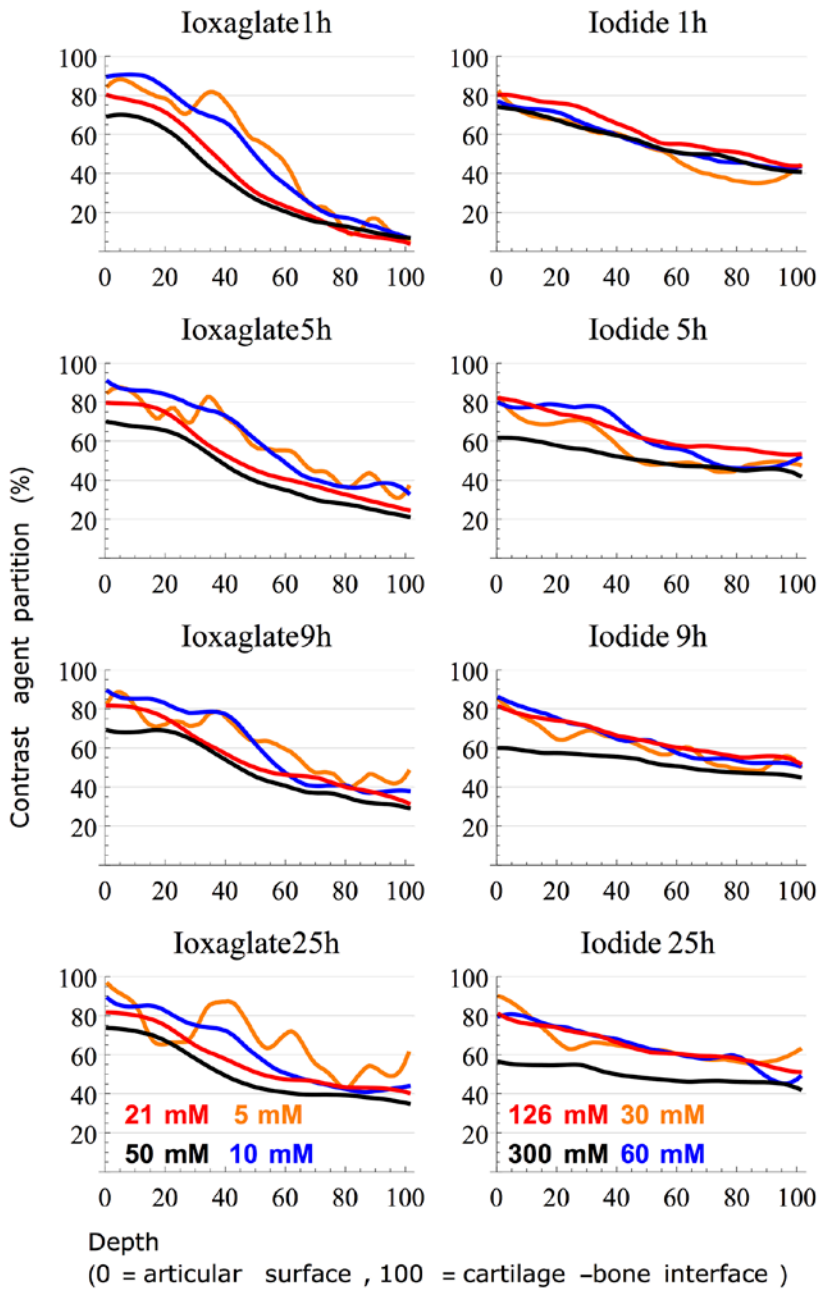

Figure 7.6: Distributions of the contrast agent (ioxaglate and iodide) concentration in bovine articular cartilage. Due to signal noise, low concentrations (orange curves) show less smooth profiles than higher concentrations.

contrast agent partitions between different concentrations of ioxaglate or iodide (Figure 7.6). However, diffusion coefficients of iodide (473 $\pm$ 133 $\mu m^2/s$) and ioxaglate (92 $\pm$ 46 $\mu m^2/s$) were significantly different ($p \leq 0.001$). In addition, at all time points, the partition coefficient of iodide was higher than the corresponding value of ioxaglate.

8 Discussion

In this study, contrast enhanced computed tomography was applied *in vitro* to examine the relationship between the diffusion properties of contrast agents with different characteristics of knee articular cartilage. Bovine and human osteochondral samples and bovine chondral discs, with intact and degenerated cartilage were used. Throughout studies I–IV, one commercial contrast agent, the anionic ioxaglate, was applied systematically to determine its diffusion rate and distribution at near equilibrium in articular cartilage. In addition, the anionic iodide, the anionic gadopentetate and the electrically neutral gadodiamide, were employed to investigate the effect of size and charge of contrast agent on diffusion into articular cartilage. To develop the CECT technique towards *in vivo* use, a clinical pQCT-scanner was used in all studies I–IV.

8.1 EFFECT OF TISSUE COMPOSITION ON CONTRAST AGENT DIFFUSION AND DISTRIBUTION

Proteoglycan content

In study I, the diffusion of ioxaglate into the superficial and middle layers of spontaneously degenerated cartilage was found to be significantly elevated. In degenerated samples, the superficial PG content was less than half of that in the intact samples and also the PG content of whole cartilage decreased. Thus, PG loss related to spontaneous degeneration of articular cartilage could be distinguished with contrast enhanced computed tomography. The loss of PGs leads to a reduction in FCD allowing the negative contrast agent to diffuse to a higher concentration in the tissue, which is the basis of the CECT and dGEMRIC methods [3,5].

It is known that in early degeneration of articular cartilage, the PG content decreases initially in the superficial and transitional zones [11]. These are the very zones where the increase in con-

trast agent intake was detected in the spontaneously degenerated cartilage. Correspondingly, earlier investigations have shown *in vitro* that artificially induced PG loss reduces FCD and negatively charged contrast agent is better able to penetrate into the cartilage [3, 4, 33, 167]. However, GAGs may not represent the entirety of the FCD within tissue. Additional contributions may come from other proteins or increased cross-linking of collagens [168, 169].

A small increase in the contrast agent concentration was discovered in the deep part of degenerated cartilage (Figure 7.2). This may be attributable either to actual degeneration in the deepest cartilage or to lowered steric hindrance of diffusion in the more superficial layers.

Solid content

Native cartilage showed increasing X-ray attenuation along the direction of tissue depth (study II). This is natural as the water content of the tissue decreases and the solid content increases towards the deep cartilage [43, 147]. The combination of PGs and collagens create a porous network and the pore size decreases from the transitional zone to deep cartilage. Thus, the X-ray attenuation corresponds to cartilage solid fraction profile in articular cartilage.

The present studies with contrast agents of different sizes and charges demonstrate that the solid matrix formed by PGs and collagen creates a steric hindrance to the diffusion of these molecules. This emerges very clearly if one examines the difference in diffusion of the contrast agent through superficial cartilage and deep cartilage (study III) *i.e.* diffusion was significantly slower through deep cartilage than through the superficial cartilage. This is consistent with reports that have pointed to an inverse relationship between the diffusion rate and the solid content of articular cartilage [134–137]. Diffusion through the cartilage-bone interface was not at a detectable level (study II), which is in agreement with earlier observations and is also supported by MRI results [36, 170].

8.2 EFFECT OF CONTRAST AGENT PROPERTIES ON DIFFUSION AND DISTRIBUTION

Size of contrast agent molecule

It requires from 12 to 24 hours for ioxaglate (M = 1269, q = -1) to achieve its diffusion equilibrium in articular cartilage (studies II-IV). Instead, with agent with smaller atomic size , it is possible to attain near equilibrium within only a few hours. The size of hydrated iodide is 0.3 nanometers [171], whereas the size of ioxaglate is 2.6 nanometers when this estimation is based on structural formula [172, 173]. The pore size of the articular cartilage ranges between 1 μm and 2 nm [35, 147, 174] and is small enough to cause significant hindrance *e.g.* for ioxaglate, but large enough to have less impact on the diffusion of atomic size iodide. As the size of a mobile molecule approaches the pore size of the medium, the freedom of movement narrows and the infiltration of the molecule slows down or is eventually prevented. In small articular cartilage samples, the tension of the PG-collagen network is at least partly relaxed and the cartilage expands. As a result of cartilage expansion, the steric hindrance may be weaker *in vitro* than *in vivo*.

Charge of the contrast agent molecule

The negative fixed charge generated by GAGs influences the diffusion of a charged contrast agent. A non-ionic contrast agent penetrates into cartilage at a greater rate and at higher amounts than a negatively charged contrast agent (study III). Correspondingly, positively charged molecules are attracted by FCD and can diffuse to higher extents than negative molecules [175, 176]. As a result, cationic contrast agents may be used at lower concentrations than anionic ones [159, 177]. In addition, cationic contrast agents have shown increased sensitivity to changes in FCD [159, 178].

In theory, a negatively charged contrast agent will distribute inversely to the spatial FCD of cartilage. Instead, the equilibrium distribution of uncharged contrast agent molecules reflects the spatial variations in the water content instead of the FCD distribution.

However, if the electron cloud of neutral molecules is polarized in the tissue, the FCD can also exert an effect. Recently synthesized new contrast agents have confirmed the importance of surface charge to the penetration properties of a contrast molecule [179]. The effect of FCD and water content of the cartilage may be difficult to separate from each other, since both tend to change towards the deep cartilage.

Theoretically, the hindrance may be weaker in the presence of repulsion than in the presence of attraction [180]. In articular cartilage, this could mean that a negative molecule of the appropriate size could diffuse more easily than a molecule of the same size but with an equivalent positive charge. In practical terms with CECT, this does not seem to be the case. For example, ioxaglate (q = -1) and contrast agent CA^{4+} molecules possess the same amount of iodine and are nearly same size with each other, as well as iothalamate (q = -1) and contrast agent CA^{1+} [175,178]. When these agents have been compared, the cationic contrast agents exhibited higher attenuation in intact articular cartilage than their anionic counterparts [175,177]. In addition, at least theoretically, spatial variations in the charge on the pore walls could even prevent diffusion completely [180]. One functional interpretation could be that in articular cartilage, spatial FCD fluctuations may induce local blockages for contrast agent or nutrient diffusion.

Concentration of the contrast agent molecule

Based on the present results, it seems that the concentration of the contrast agent does not influence interpretation of the CECT images, which is beneficial for clinical applicability of CECT. Diffusion or partition of the contrast agent in articular cartilage did not change with different concentration (study IV). This is somewhat surprising as in theory concentration can affect diffusion. On the other hand, concentration dependence usually does not appear in diluted solutions [119,181], which is typically the case in biology. In the present study, contrast agents were in the concentration range of 5-300 mM. The present results are in agreement with Torzilli,

who used glucose and dextran in a concentration range of 0.25-25 mM [182].

In contrast to the present findings, a reduction of the concentration of negative contrast agent has been reported to decrease its sensitivity to changes in FCD, or even lose the trend of inverse proportionality with GAG [5,159,175]. Similarly, a low concentration of a cationic contrast agent CA^{4+} has been reported to poorly reflect the GAG distribution when this is evaluated by CECT [178].

8.3 FUTURE OF CECT

In an ideal case, CECT is capable of achieving the simultaneous imaging of cartilage, meniscus and bone [183, 184], as well as enabling the segmentation of cartilage and subchondral bone and providing a quantitative analysis of bone structure and integrity of articular cartilage and meniscus.

Clinical investigations indicate that the half-life of contrast agent in joint space is less than one hour [6, 7], which is not long enough for the agent to be able to reach diffusion equilibrium in the articular cartilage of the human knee. By measuring the diffusion rate of contrast agent, it is possible to distinguish degenerated cartilage from intact tissue. However, this necessitates two or more CECT scans, inevitably increasing the radiation dose. Accurate segmentation of tissues and measurement of contrast agent diffusion requires imaging both immediately after contrast agent administration and after a delay, typically from 30 to 60 minutes [2, 6, 7, 185]. However, two or more CECT scans could be avoided by using a mixture of contrast agents, one which would remain in the joint space and the other would diffuse into cartilage. Furthermore, dual energy CT scans could enhance tissue segmentation and be advantageous in the determination of the contrast agent content in articular cartilage.

The remaining challenges include the determination of the threshold of an increase in the contrast which would be considered as being diagnostic of degeneration of articular cartilage and agree-

ment on standard imaging times, as well as on the optimal delay between contrast administration and imaging. In addition, the currently available clinical contrast agents may be harmful to patients [156,186]. The development of new contrast agents could not only reduce toxicity but hopefully also improve attenuation and sensitivity in imaging [158,175].

In conclusion, in the future, the X-ray phase-contrast CECT may be the next revolution in the clinical imaging of articular cartilage [187, 188], especially when combined with sophisticated 3D biomechanical models in the assessment of joint function and prognosis of OA development [189,190].

9 Summary and conclusions

The present results indicate that CECT can be used with a clinical pQCT scanner to diagnose PG depletion in spontaneously degenerated articular cartilage. There are differences in the equilibrium distributions of contrast agent in an intact and degenerated articular cartilage. Since cartilage degeneration begins at the articular surface, in comparison to the situation in intact cartilage, more contrast agent is able to accumulate in the superficial part of cartilage if there is the presence of early OA.

The equilibrium distribution of a negatively charged contrast agent displays a negative correlation with that of the PGs. Although PGs are mostly responsible for the distribution of the contrast agent in articular cartilage, also water and collagen distributions influence this parameter. However, diffusion equilibrium is not reached until at least 24 hours in human knee articular cartilage, except with molecules with atomic sizes. This means that diffusion equilibrium cannot be reached within clinical imaging times using the currently available clinical contrast agents.

An increase in the molecular size of contrast agent caused an increase in steric hindrance attributable to the articular cartilage matrix. However, it was found that the concentration of the contrast agent did not affect the agent's diffusion or partition in articular cartilage. Clinically this is important since it means that individual variations in contrast agent concentrations will not compromise the diagnostic reliability of CECT imaging.

Bibliography

[1] L. Andrén and L. Wehlin, "Double-contrast arthrography of knee with horizontal roentgen ray beam," *Acta Orthop* **29,** 307–314 (1959).

[2] M. W. Spring and J. C. Buckland-Wright, "Contrast medium imbibition in osteoarthritic cartilage," *Brit J Radiol* **63,** 823–825 (1990).

[3] A. Bashir, M. L. Gray, and D. Burstein, "Gd-DTPA2- as a measure of cartilage degradation," *Magn Reson Med* **36,** 665–673 (1996).

[4] M. D. Cockman, C. A. Blanton, P. A. Chmielewski, L. Dong, T. E. Dufresne, E. B. Hookfin, M. J. Karb, S. Liu, and K. R. Wehmeyer, "Quantitative imaging of proteoglycan in cartilage using a gadolinium probe and microCT," *Osteoarthritis Cartilage* **14,** 210–214 (2006).

[5] A. W. Palmer, R. E. Guldberg, and M. E. Levenston, "Analysis of cartilage matrix fixed charge density and three-dimensional morphology via contrast-enhanced microcomputed tomography," *Proc Natl Acad Sci USA* **103,** 19255–19260 (2006).

[6] H. T. Kokkonen, A. S. Aula, H. Kröger, J.-S. Suomalainen, E. Lammentausta, E. Mervaala, J. S. Jurvelin, and J. Töyräs, "Delayed computed tomography arthrography of human knee cartilage in vivo," *Cartilage* **3,** 334–341 (2012).

[7] H. T. Kokkonen, J.-S. Suomalainen, A. Joukainen, H. Kröger, J. Sirola, J. S. Jurvelin, J. Salo, and J. Töyräs, "In vivo diagnostics of human knee cartilage lesions using delayed CBCT arthrography," *J Orthop Res* **32,** 403–412 (2014).

[8] A. J. Bollet and J. L. Nance, "Biochemical findings in normal and osteoarthritic articular cartilage. II. Chondroitin sulfate concentration and chain length, water, and ash content," *J Clin Invest* **45,** 1170–1177 (1966).

[9] C. G. Armstrong and V. C. Mow, "Variations in the intrinsic mechanical properties of human articular cartilage with age, degeneration, and water content," *J Bone Joint Surg Am* **64,** 88–94 (1982).

[10] J. A. Buckwalter and H. J. Mankin, "Instructional course lectures, The American Academy of Orthopaedic Surgeons - Articular cartilage. Part I: Tissue design and chondrocyte-matrix interactions," *J Bone Joint Surg Am* **79,** 600–611 (1997).

[11] J. A. Buckwalter and H. J. Mankin, "Instructional course lectures, The American Academy of Orthopaedic Surgeons - Articular cartilage. Part II: Degeneration and osteoarthrosis, repair, regeneration, and transplantation," *J Bone Joint Surg Am* **79-A,** 612–632 (1997).

[12] S. Saarakkala, M. S. Laasanen, J. S. Jurvelin, K. Torronen, M. J. Lammi, R. Lappalainen, and J. Toyras, "Ultrasound indentation of normal and spontaneously degenerated bovine articular cartilage," *Osteoarthritis Cartilage* **11,** 697–705 (2003).

[13] W. Wilson, C. van Burken, C. van Donkelaar, P. Buma, B. van Rietbergen, and R. Huiskes, "Causes of mechanically induced collagen damage in articular cartilage," *J Orthop Res* **24,** 220–228 (2006).

[14] I. Kiviranta, M. Tammi, J. Jurvelin, J. Arokoski, A. M. Saamanen, and H. J. Helminen, "Articular cartilage thickness and glycosaminoglycan distribution in the young canine knee joint after remobilization of the immobilized limb," *J Orthop Res* **12,** 161–167 (1994).

[15] L. Lippiello, D. Hall, and H. J. Mankin, "Collagen synthesis in normal and osteoarthritic human cartilage," *J Clin Invest* **59,** 593–600 (1977).

[16] F. Nelson, L. Dahlberg, S. Laverty, A. Reiner, I. Pidoux, M. Ionescu, G. L. Fraser, E. Brooks, M. Tanzer, L. C. Rosenberg, P. Dieppe, and A. R. Poole, "Evidence for altered synthesis of type II collagen in patients with osteoarthritis," *J Clin Invest* **102,** 2115–2125 (1998).

[17] V. B. Kraus, T. B. Kepler, T. Stabler, J. Renner, and J. Jordan, "First qualification study of serum biomarkers as indicators of total body burden of osteoarthritis," *PLoS ONE* **5,** e9739 (2010).

[18] N. Arden and M. C. Nevitt, "Osteoarthritis: epidemiology," *Best Pract Res Clin Rheumatol* **20,** 3–25 (2006).

[19] D. T. Felson, "Developments in the clinical understanding of osteoarthritis," *Arthritis Res Ther* **11,** 203 (2009).

[20] J. W.-P. Michael, K. U. Schlüter-Brust, and P. Eysel, "The epidemiology, etiology, diagnosis, and treatment of osteoarthritis of the knee," *Dtsch Arztebl Int* **107,** 152–162 (2010).

[21] WHO, "The global burden of disease: 2004 update," Web page www.who.int/healthinfo/global burden disease/2004 report update (2008).

[22] WHO, "Programmes: Chronic diseases and health promotion," Web page www.who.int/entity/en/ (checked 26.3.2015) (2015).

[23] M. H. Atkinson, "Osteoarthrosis," *Can Fam Physician* **30,** 1503–1507 (1984).

[24] D. M. Salter, "Degenerative joint disease," *Current Diagnostic Pathology* **8,** 11–18 (2002).

[25] G. Li, J. Yin, J. Gao, T. S. Cheng, N. J. Pavlos, C. Zhang, and M. H. Zheng, "Subchondral bone in osteoarthritis: insight into risk factors and microstructural changes," *Arthritis Res Ther* **15,** 223 (2013).

[26] T. R. McAdams, K. Mithoefer, J. M. Scopp, and B. R. Mandelbaum, "Articular cartilage injury in athletes," *Cartilage* **1,** 165–179 (2010).

[27] Y.-M. Kim and Y.-B. Joo, "Patellofemoral osteoarthritis," *Knee Surg Relat Res* **24,** 193–200 (2012).

[28] T. E. McAlindon, R. R. Bannuru, M. C. Sullivan, N. K. Arden, F. Berenbaum, S. M. Bierma-Zeinstra, G. A. Hawker, Y. Henrotin, D. J. Hunter, H. Kawaguchi, K. Kwoh, S. Lohmander, F. Rannou, E. M. Roos, and M. Underwood, "OARSI guidelines for the non-surgical management of knee osteoarthritis," *Osteoarthritis and Cartilage* **22,** 363–388 (2014).

[29] S. Knecht, B. Vanwanseele, and E. Stussi, "A review on the mechanical quality of articular cartilage - implications for the diagnosis of osteoarthritis," *Clin Biomech (Bristol, Avon)* **21,** 999–1012 (2006).

[30] C. W. Hayes and W. F. Conway, "Evaluation of articular cartilage: Radiographic and cross-sectional imaging techniques," *RadioGraphics* **12,** 409–428 (1992).

[31] T. J. Colegate-Stone and P. Allen, "Can plain radiography accurately predict the arthroscopic findings of articular knee cartilage - A prospective study," *J Bone Joint Surg Br* **91-B,** 421 (2009).

[32] A. Bashir, M. L. Gray, R. D. Boutin, and D. Burstein, "Glycosaminoglycan in articular cartilage: in vivo assessment with delayed Gd(DTPA)(2-)-enhanced MR imaging," *Radiology* **205,** 551–558 (1997).

[33] A. S. Kallioniemi, J. S. Jurvelin, M. T. Nieminen, M. J. Lammi, and J. Toyras, "Contrast agent enhanced pQCT of articular cartilage," *Phys Med Biol* **52,** 1209–1219 (2007).

[34] P. J. Roughley, "The structure and function of cartilage proteoglycans," *Eur Cell Mater* **12,** 92–101 (2006).

[35] V. C. Mow, A. Ratcliffe, and A. R. Poole, "Cartilage and diarthrodial joints as paradigms for hierarchical materials and structures," *Biomaterials* **13,** 67–97 (1992).

[36] A. Maroudas, P. Bullough, S. A. Swanson, and M. A. Freeman, "The permeability of articular cartilage," *J Bone Joint Surg Br* **50,** 166–177 (1968).

[37] D. E. T. Shepherd and B. B. Seedhom, "Thickness of human articular cartilage in joints of the lower limb," *Ann Rheum Dis* **58,** 27–34 (1999).

[38] T. M. Quinn, E. B. Hunziker, and H.-J. Häuselmann, "Variation of cell and matrix morphologies in articular cartilage among locations in the adult human knee," *OsteoArthritis and Cartilage* **13,** 672–678 (2005).

[39] B. Möller, H. Bonel, M. Rotzetter, P. M. Villiger, and H.-R. Ziswiler, "Measuring finger joint cartilage by ultrasound as a promising alternative to conventional radiograph imaging," *Arthritis and Rheumatism* **61,** 435–441 (2009).

[40] H. A. Alhadlaq, Y. Xia, J. B. Moody, and J. R. Matyas, "Detecting structural changes in early experimental osteoarthritis of tibial cartilage by microscopic magnetic resonance imaging and polarized light microscopy," *Ann Rheum Dis* **63,** 709–717 (2004).

[41] E. B. Hunziker, T. M. Quinn, and H.-J. Häuselmann, "Quantitative structural organization of normal adult human articular cartilage," *Osteoarthritis and Cartilage* **10,** 564–572 (2002).

[42] C. Weiss, L. Rosenberg, and A. J. Helfet, "An ultrastructural study of normal young adult human articular cartilage," *J Bone Joint Surg Am* **50,** 663–674 (1968).

[43] M. Venn and A. Maroudas, "Chemical composition and swelling of normal and osteoarthrotic femoral head cartilage I. Chemical composition," *Ann Rheum Dis* **36,** 121–129 (1977).

[44] N. D. Broom and C. A. Poole, "A functional-morphological study of the tidemark region of articular cartilage maintained in a non-viable physical condition," *J Anat* **135,** 65–82 (1982).

[45] T. R. Oegema, R. J. Carpenter, F. Hofmeister, and R. C. Thompson, "The interaction of the zone of calcified cartilage and subchondral bone in osteoarthritis," *Microsc Res Tech* **37,** 324–332 (1997).

[46] P. L. Mente and J. L. Lewis, "Elastic modulus of calcified cartilage is an order of magnitude less than that of subchondral bone," *J Orthop Res* **12,** 637–647 (1994).

[47] A. K. Jeffery, G. W. Blunn, C. W. Archer, and G. Bentley, "Three-dimensional collagen architecture in bovine articular cartilage," *J Bone Joint Surg Br* **73,** 795–801 (1991).

[48] M. J. Kaab, I. A. Gwynn, and H. P. Notzli, "Collagen fibre arrangement in the tibial plateau articular cartilage of man and other mammalian species," *J Anat* **193 (Pt 1,** 23–34 (1998).

[49] C. Muehleman, S. Majumdar, A. S. Issever, F. Arfelli, R.-H. Menk, L. Rigon, G. Heitner, B. Reime, J. Metge, A. Wagner, K. E. Kuettner, and J. Mollenhauer, "X-ray detection of structural orientation in human articular cartilage," *OsteoArthritis and Cartilage* **12,** 97–105 (2004).

[50] J. M. Lane and C. Weiss, "Review of articular cartilage collagen research," *Arthritis and Rheumatism* **18,** 553–562 (1975).

[51] R. J. Minns and F. S. Steven, "The collagen fibril organization in human articular cartilage," *J Anat* **123,** 437–457 (1977).

[52] D. R. Eyre, M. A. Weiss, and J.-J. Wu, "Articular cartilage collagen: An irreplaceable framework?," *Eur Cell Mater* **12,** 57–63 (2006).

[53] J.-J. Wu, M. A. Weiss, L. S. Kim, and D. R. Eyre, "Type III collagen, a fibril network modifier in articular cartilage," *J Biol Chem* **285,** 18537–18544 (2010).

[54] B. Alberts, A. Johnson, J. Lewis, M. Raff, K. Roberts, and P. Walter, *Molecular biology of the cell*, 4th ed. (Garland Science, New York, 2002).

[55] A. K. Williamson, A. C. Chen, K. Masuda, E. J.-M. A. Thonar, and R. L. Sah, "Tensile mechanical properties of bovine articular cartilage: variations with growth and relationships to collagen network components," *J Orthop Res* **21,** 872–880 (2003).

[56] S. Hosseininia, L. R. Lindberg, and L. E. Dahlberg, "Cartilage collagen damage in hip osteoarthritis similar to that seen in knee osteoarthritis; a case-control study of relationship between collagen, glycosaminoglycan and cartilage swelling," *BMC Musculoskelet Disord* **14,** 18 (2013).

[57] A. P. Hollander, T. F. Heathfield, C. Webber, Y. Iwata, R. Bourne, C. Rorabeck, and A. R. Poole, "Increased damage to type II collagen in osteoarthritic articular cartilage detected by a new immunoassay," *J Clin Invest* **93,** 1722–1732 (1994).

[58] J. Toyras, M. S. Laasanen, S. Saarakkala, M. J. Lammi, J. Rieppo, J. Kurkijarvi, R. Lappalainen, and J. S. Jurvelin, "Speed of sound in normal and degenerated bovine articular cartilage," *Ultrasound Med Biol* **29,** 447–454 (2003).

[59] H. A. Kim, S. D-I, and Y. W. Song, "Relationship between chondrocyte apoptosis and matrix depletion in human articular cartilage," *J Rheumatol* **28,** 2038–2045 (2001).

[60] K. D. Jadin, W. C. Bae, B. L. Schumacher, and R. L. Sah, "Three-dimensional (3-D) imaging of chondrocytes in articular cartilage: Growth-associated changes in cell organization," *Biomaterials* **28,** 230–239 (2007).

[61] M. F. Venn, "Chemical composition of human femoral head cartilage: influence of topographical position and fibrillation," *Annals of the Rheumatic Diseases* **38,** 57–62 (1979).

[62] S. S. Chen, Y. H. Falcovitz, R. Schneiderman, A. Maroudas, and R. L. Sah, "Depth-dependent compressive properties of normal aged human femoral head articular cartilage: relationship to fixed charge density," *OsteoArthritis and Cartilage* **9,** 561–569 (2001).

[63] I. Kiviranta, J. Jurvelin, M. Tammi, A. M. Saamanen, and H. J. Helminen, "Microspectrophotometric quantitation of glycosaminoglycans in articular cartilage sections stained with Safranin O," *Histochemistry* **82,** 249–255 (1985).

[64] J. A. Buckwalter and H. J. Mankin, "Articular cartilage: tissue design and chondrocyte-matrix interactions," *Instr Course Lect* **47,** 477–486 (1998).

[65] A. Maroudas, M. T. Bayliss, and M. F. Venn, "Further studies on the composition of human femoral head cartilage," *Ann Rheum Dis* **39,** 514–523 (1980).

[66] T. E. Hardingham and A. J. Fosang, "Proteoglycans: many forms and many functions," *FASEB J* **6,** 861–870 (1992).

[67] P. G. Bush and A. C. Hall, "The volume and morphology of chondrocytes within non-degenerate and degenerate human articular cartilage," *OsteoArthritis and Cartilage* **11,** 242–251 (2003).

[68] K. Huch, "Knee and ankle: human joints with different susceptibility to osteoarthritis reveal different cartilage cellular-

ity and matrix synthesis in vitro," *Arch Orthop Trauma Surg* **121,** 301–306 (2001).

[69] M. Lotz and R. F. Loeser, "Effects of aging on articular cartilage homeostasis," *Bone* **51,** 241–248 (2012).

[70] J. A. Buckwalter, L. C. Rosenberg, and E. B. Hunziker, "Articular cartilage: Composition, structure, response to injury, and methods of facilitating repair," in *Articular cartilage and knee joint function: Basic science and arthroscopy*, J. W. Ewing, ed. (Raven Press Ltd., New York, 1990), pp. 19–56.

[71] F. Lei and A. Z. Szeri, "The influence of fibril organization on the mechanical behaviour of articular cartilage," *Proc R Soc A* **462,** 3301–3322 (2006).

[72] A. J. Grodzinsky, "Electromechanical and physicochemical properties of connective tissue," *CRC Critical Reviews in Biomedical Engineering* **9,** 133–199 (1983).

[73] N. P. Cohen, R. J. Foster, and V. C. Mow, "Composition and dynamics of articular cartilage: structure, function, and maintaining healthy state," *J Orthop Sports Phys Ther* **28,** 203–215 (1998).

[74] N. M. Bachrach, V. C. Mow, and F. Guilak, "Incompressibility of the solid matrix of articular cartilage under high hydrostatic pressures," *J Biomech* **31,** 445–451 (1998).

[75] L. P. Li, W. Herzog, R. K. Korhonen, and J. S. Jurvelin, "The role of viscoelasticity of collagen fibers in articular cartilage: axial tension versus compression," *Med Eng Phys* **27,** 51–57 (2005).

[76] A. Oloyede, R. Flachsmann, and N. D. Broom, "The dramatic influence of loading velocity on the compressive response of articular cartilage," *Connect Tissue Res* **27,** 211–224 (1992).

[77] S. Park, C. T. Hung, and G. A. Ateshian, "Mechanical response of bovine articular cartilage under dynamic unconfined compression loading at physiological stress levels," *Osteoarthritis Cartilage* **12,** 65–73 (2004).

[78] J. S. Jurvelin, M. D. Buschmann, and E. B. Hunziker, "Mechanical anisotropy of the human knee articular cartilage in compression," *Proc Instn Mech Engrs* **217,** 215–219 (2003).

[79] S. Chegini and S. J. Ferguson, "Time and depth dependent Poisson's ratio of cartilage explained by an inhomogeneous orthotropic fiber embedded biphasic model," *J Biomech* **43,** 1660–1666 (2010).

[80] C.-Y. Huang, V. C. Mow, and G. A. Ateshian, "The role of flow-independent viscoelasticity in the biphasic tensile and compressive responses of articular cartilage," *J Biomech Eng* **123,** 410–417 (2001).

[81] M. M. Temple, W. C. Bae, M. Q. Chen, M. Lotz, D. Amiel, R. D. Coutts, and R. L. Sah, "Age- and site-associated biomechanical weakening of human articular cartilage of the femoral condyle," *OsteoArthritis and Cartilage* **15,** 1042–1052 (2007).

[82] B. J. Ewers, D. Dvoracek-Driksna, M. W. Orth, and R. C. Haut, "The extent of matrix damage and chondrocyte death in mechanically traumatized articular cartilage explants depends on rate of loading," *J Orthop Res* **19,** 779–784 (2001).

[83] R. B. Salter and P. Field, "The effects of continuous compression on living articular cartilage," *J Bone Joint Surg Am* **42,** 31–90 (1960).

[84] A. Trias, "Effect of persistent pressure on the articular cartilage: An experimental study," *J Bone Joint Surg* **43B,** 376–386 (1961).

[85] T. D. Spector and A. J. MacGregor, "Risk factors for osteoarthritis: genetics," *OsteoArthritis and Cartilage* **12,** S39–S44 (2004).

[86] H. J. Mankin, "The response of articular cartilage to mechanical injury," *J Bone Joint Surg Am* **64,** 460–466 (1982).

[87] L. S. Lohmander, L. M. Atley, T. A. Pietka, and D. R. Eyre, "The release of crosslinked peptides from type II collagen into human synovial fluid is increased soon after joint injury and in osteoarthritis," *Arthritis and Rheumatism* **48,** 3130–3139 (2003).

[88] D. Ishimaru, N. Sugiura, H. Akiyama, H. Watanabe, and K. Matsumoto, "Alterations in the chondroitin sulfate chain in human osteoartritic cartilage of the knee," *Osteoarthritis and Cartilage* **22,** 250–258 (2014).

[89] G. Rizkalla, A. Reiner, E. Bogoch, and A. R. Poole, "Studies of the articular cartilage proteoglycan aggrecan in health and osteoarthritis: Evidence for molecular heterogeneity and extensive molecular changes in disease," *J Clin Invest* **90,** 2268–2277 (1992).

[90] L. J. Sandell and T. Aigner, "Articular cartilage and changes in arthritis. An introduction: Cell biology of osteoarthritis," *Arthritis Res* **3,** 107–113 (2001).

[91] M. K. Lotz, S. Otsuki, S. P. Grogan, R. Sah, R. Terkeltaub, and D. D'Lima, "Cartilage cell clusters," *Arthritis Rheum* **62,** 2206–2218 (2010).

[92] Y. Sun, D. R. Mauerhan, P. R. Honeycutt, J. S. Kneisl, H. J. Norton, N. Zinchenko, E. N. Hanley, and H. E. Gruber, "Calcium deposition in osteoarthritic meniscus and meniscal cell culture," *Arthritis Res Ther* **12,** R56 (2010).

[93] J. S. Thomsen, T. S. Straarup, C. C. Danielsen, H. Oxlund, and A. Brüel, "Relationship between articular cartilage damage

and subchondral bone properties and meniscal ossification in the Dunkin Hartley guinea pig model of osteoarthritis," *Scand J Rheumatol* **40,** 391–399 (2011).

[94] H. Mitsuyama, R. M. Healey, R. A. Terkeltaub, R. D. Coutts, and D. Amiel, "Calcification of human articular knee cartilage is primarily an effect of aging rather than osteoarthritis," *OsteoArthritis and Cartilage* **15** (2006).

[95] I. Kiviranta, J. Jurvelin, M. Tammi, A. M. Saamanen, and H. J. Helminen, "Weight bearing controls glycosaminoglycan concentration and articular cartilage thickness in the knee joints of young beagle dogs," *Arthritis Rheum* **30,** 801–809 (1987).

[96] D. T. Felson, J. Niu, A. Guermazi, B. Sack, and P. Aliabadi, "Defining radiographic incidence and progression of knee osteoarthritis: suggested modifications of the Kellgren and Lawrence scale," *Ann Rheum Dis* **70,** 1884–1886 (2011).

[97] A. Guermazi, D. Hayashi, F. Eckstein, D. J. Hunter, J. Duryea, and F. W. Roemer, "Imaging of osteoarthritis," *Rheum Dis Clin N Am* **39,** 67–105 (2013).

[98] G. Spahn, H. M. Klinger, and G. O. Hofmann, "How valid is the arthroscopic diagnosis of cartilage lesions? Results of an opinion survey among highly experienced arthroscopic surgeons," *Arch Orthop Trauma Surg* **129,** 1117–1121 (2009).

[99] S. Saarakkala, P. Waris, V. Waris, I. Tarkiainen, E. Karvanen, J. Aarnio, and J. M. Koski, "Diagnostic performance of knee ultrasonography for detecting degenerative changes of articular cartilage," *Osteoarthritis and Cartilage* **20,** 376–381 (2012).

[100] C. G. Peterfy, G. Gold, F. Eckstein, F. Cicuttini, B. Dardzinski, and R. Stevens, "MRI protocols for whole-organ assessment of the knee in osteoarthritis," *OsteoArthritis and Cartilage* **14,** A95–A111 (2006).

[101] S. Trattnig, S. Domayer, G. W. Welsch, T. Mosher, and F. Eckstein, "MR imaging of cartilage and its repair in the knee - a review," *Eur Radiol* **19,** 1582–1594 (2009).

[102] J. H. Kellgren and J. S. Lawrence, "Radiological assessment of osteo-arthrosis," *Ann Rheum Dis* **16,** 494–502 (1957).

[103] J. Henckel, R. Richards, K. Lozhkin, S. Harris, F. M. Rodriguez y Baena, A. R. W. Barrett, and J. P. Cobb, "Very low-dose computed tomography for planning and outcome measurement in knee replacement," *J Bone Joint Surg Br* **88-B,** 1513–1518 (2006).

[104] P. Simoni, P.-P. Leyder, A. Albert, F. Malchair, C. Maréchal, L. Scarciolla, B. B. Zobel, V. A. Miezentseva, and P. Gillet, "Optimization of computed tomography (CT) arthrography of hip for the visualization of cartilage: an in vitro study," *Skeletal Radiol* **43,** 169–178 (2014).

[105] STUK, "Suomalaisen keskimääräinen säteilyannos," Web page www.stuk.fi/aiheet/mita-sateily-on/ihmisen-radioaktiivisuus/suomalaisen-keskimaarainen-sateilyannos (2015).

[106] R. K. Korhonen, M. Wong, J. Arokoski, R. Lindgren, H. J. Helminen, E. B. Hunziker, and J. S. Jurvelin, "Importance of the superficial tissue layer for the indentation stiffness of articular cartilage," *Med Eng Phys* **24,** 99–108 (2002).

[107] E. Kaleva, T. Virén, S. Saarakkala, J. Sahlman, J. Sirola, J. Puhakka, T. Paatela, H. Kröger, I. Kiviranta, J. S. Jurvelin, and J. Töyräs, "Arthroscopic ultrasound assessment of articular cartilage in the human knee joint: A potential diagnostic method.," *Cartilage* **2,** 246–253 (2011).

[108] T. Virén, Y. P. Huang, S. Saarakkala, H. Pulkkinen, V. Tiitu, A. Linjama, I. Kiviranta, M. J. Lammi, A. Brünott, H. Brommer, R. Van Weeren, P. A. J. Brama, Y. P. Zheng, J. S. Jurvelin,

and J. Töyräs, "Comparison of ultrasound and optical coherence tomography techniques for evaluation of integrity of spontaneously repaired horse cartilage," *J Med Eng Technol* **36,** 185–192 (2012).

[109] M. A. D'Agostino, P. Conaghan, M. Le Bars, G. Baron, W. Grassi, E. Martin-Mola, R. Wakefield, J.-L. Brasseur, A. So, M. Backhaus, M. Malaise, G. Burmester, N. Schmidely, P. Ravaud, M. Dougados, and P. Emery, "EULAR report on the use of ultrasonography in painful knee osteoarthritis. Part 1: Prevalence of inflammation in osteoarthritis," *Ann Rheum Dis* **64,** 1703–1709 (2005).

[110] M. D. Crema, F. W. Roemer, M. D. Marra, D. Burstein, G. E. Gold, F. Eckstein, T. Baum, T. Mosher, J. A. Carrino, and A. Guermazi, "Articular cartilage in the knee: current MR imaging techniques and applications in clinical practice and research," *RadioGraphics* **31,** 37–62 (2011).

[111] M. T. Nieminen, J. Rieppo, J. Töyräs, J. M. Hakumäki, J. Silvennoinen, M. M. Hyttinen, H. J. Helminen, and J. S. Jurvelin, "T2 relaxation reveals spatial collagen architecture in articular cartilage: A comparative quantitative MRI and polarized light microscopic study," *Magnetic Resonance in Medicine* **46,** 487–493 (2001).

[112] D. J. Dowsett, P. A. Kenny, and E. R. Johnston, *The Physics of Diagnostic Imaging*, 2nd ed. (Hodder Arnold, 2006).

[113] D. Burstein, J. Velyvis, K. T. Scott, K. W. Stock, Y.-J. Kim, D. Jaramillo, R. D. Boutin, and M. L. Gray, "Protocol issues for delayed Gd(DTPA)2- -enhanced MRI (dGEMRIC) for clinical evaluation of articular cartilage," *Magn Reson Med* **45,** 36–41 (2001).

[114] C. J. Tiderius, R. Jessel, Y.-J. Kim, and D. Burstein, "Hip dGEMRIC in asymptomatic volunteers and patients with

early osteoarthritis: The influence of timing after contrast injection," *Magn Reson Med* **57,** 803–805 (2007).

[115] J. Hirvasniemi, K. A. M. Kulmala, E. Lammentausta, R. Ojala, P. Lehenkari, A. Kamel, J. S. Jurvelin, J. Töyräs, M. T. Nieminen, and S. Saarakkala, "In vivo comparison of delayed gadolinium-enhanced MRI of cartilage and delayed quantitative CT arthrography in imaging of articular cartilage," *Osteoarthritis and Cartilage* **21,** 434–442 (2013).

[116] F. Eckstein, M. Hudelmaier, and R. Putz, "The effects of exercise on human articular cartilage," *J Anat* **208,** 491–512 (2006).

[117] S. Trattnig, S. Marlovits, S. Gebetsroither, P. Szomolanyi, G. H. Welsch, E. Salomonowitz, A. Watanabe, M. Deimling, and T. C. Mamisch, "Three-dimensional delayed gadolinium-enhanced MRI of cartilage (dGEMRIC) for in vivo evaluation of reparative cartilage after matrix-associated autologous chondrocyte transplantation at 3.0T: Preliminary results," *J Magn Reson Imaging* **26,** 974–982 (2007).

[118] E. M. Roos and L. Dahlberg, "Positive effects of moderate exercise on glycosaminoglycan content in knee cartilage: A four-month, randomized, controlled trial in patients at risk of osteoarthritis," *Arthritis and Rheumatism* **52,** 3507–3514 (2005).

[119] J. Crank, *The mathematics of diffusion*, 2nd ed. (Oxford University Press, New York, 1975).

[120] M. H. Jacobs, *Diffusion processes* (Springer-Verlag, Berlin, 1967).

[121] R. B. Bird, W. E. Stewart, and E. N. Lightfoot, *Transport Phenomena*, 2nd ed. (John Wiley and Sons, 2007).

[122] H. Mehrer and N. A. Stolwijk, "Heroes and highlights in the history of diffusion," *Diffusion Fundamentals* **11,** 1–32 (2009).

[123] E. L. Cussler, *Diffusion. Mass transfer in fluid systems*, 3rd ed. (Cambridge University Press, 2009).

[124] G. Arfken, *Mathematical methods for physicists*, 3rd ed. (Academic Press, San Diego, 1985).

[125] F. G. Donnan, "The theory of membrane equilibria," *Chem Rev* **1,** 73–90 (1924).

[126] A. Maroudas and H. Evans, "A study of ionic equilibria in cartilage," *Connect Tissue Res* **1,** 69–77 (1972).

[127] B. P. O'Hara, J. P. G. Urban, and A. Maroudas, "Influence of cyclic loading on the nutrition of articular cartilage," *Ann Rheum Dis* **49,** 536–539 (1990).

[128] S. Rajasekaran, J. Naresh-Babu, and S. Murugan, "Review of postcontrast MRI studies on diffusion of human lumbar discs," *J Magn Reson Imaging* **25,** 410–418 (2007).

[129] H. A. Horner and J. P. G. Urban, "2001 Volvo Award winner in basic science studies: effect of nutrient supply on the viability of cells from the nucleus pulposus of the intervertebral disc," *Spine* **26,** 2543–2549 (2001).

[130] É. Sélard, A. Shirazi-Adl, and J. P. G. Urban, "Finite element study of nutrient diffusion in the human intervertebral disc," *Spine* **28,** 1945–1953 (2003).

[131] A. Shirazi-Adl, M. Taheri, and J. P. G. Urban, "Analysis of cell viability in intervertebral disc: effect of endplate permeability on cell population," *J Biomech* **43,** 1330–1336 (2010).

[132] K. Kräuchi, "How is the circadian rhythm of core body temperature regulated?," *Clin Auton Res* **12,** 147–149 (2002).

[133] T. M. Quinn, P. Kocian, and J.-J. Meister, "Static compression is associated with decreased diffusivity of dextrans in cartilage explants," *Arch Biochem Biophys* **384,** 327–334 (2000).

[134] L. Zhang and A. Z. Szeri, "Transport of neutral solute in articular cartilage: effect of microstructure anisotropy," *J Biomech* **41,** 430–437 (2008).

[135] K. P. Arkill and C. P. Winlove, "Solute transport in the deep and calcified zones of articular cartilage," *Osteoarthritis Cartilage* **16,** 708–714 (2008).

[136] R. C. Evans and T. M. Quinn, "Solute diffusivity correlates with mechanical properties and matrix density of compressed articular cartilage," *Arch Biochem Biophys* **442,** 1–10 (2005).

[137] H. A. Leddy and F. Guilak, "Site-specific molecular diffusion in articular cartilage measured using fluorescence recovery after photobleaching," *Ann Biomed Eng* **31,** 753–760 (2003).

[138] A. Maroudas, "Distribution and diffusion of solutes in articular cartilage," *Biophys J* **10,** 365–379 (1970).

[139] E. Nimer, R. Schneiderman, and A. Maroudas, "Diffusion and partition of solutes in cartilage under static load," *Biophys Chem* **106,** 125–146 (2003).

[140] T. M. Piscaer, J. H. Waarsing, N. Kops, P. Pavljasevic, J. A. Verhaar, G. J. van Osch, and H. Weinans, "In vivo imaging of cartilage degeneration using microCT-arthrography," *Osteoarthritis Cartilage* **16,** 1011–1017 (2008).

[141] S. Roberts, J. P. Urban, H. Evans, and S. M. Eisenstein, "Transport properties of the human cartilage endplate in relation to its composition and calcification," *Spine* **21,** 415–420 (1996).

[142] J. Wellen, K. G. Helmer, P. Grigg, and C. H. Sotak, "Application of porous-media theory to the investigation of water ADC changes in rabbit achilles tendon caused by tensile loading," *J Magn Reson* **170,** 49–55 (2004).

[143] P. J. Basser, "Inferring microstructural features and the physiological state of tissues from diffusion-weighted images," *NMR Biomed* **8,** 333–344 (1995).

[144] A. Maroudas, "Physicochemical properties of cartilage in the light of ion exchange theory," *Biophys J* **8,** 575–595 (1968).

[145] A. Maroudas, "Biophysical chemistry of cartilaginous tissues with special reference to solute and fluid transport," *Biorheology* **12,** 233–248 (1975).

[146] A. Maroudas, "Transport of solutes through cartilage: permeability to large molecules," *J Anat* **122,** 335–347 (1976).

[147] V. C. Mow, M. H. Holmes, and W. M. Lai, "Fluid transport and mechanical properties of articular cartilage: a review," *J Biomech* **17,** 377–394 (1984).

[148] M. Y. Kiriukhin and K. D. Collins, "Dynamic hydration numbers for biologically important ions," *Biophys Chem* **99,** 155–168 (2002).

[149] J. Zhou, X. Lu, Y. Wang, and J. Shi, "Molecular dynamics study on ionic hydration," *Fluid Phase Equilibria* **194-197,** 257–270 (2002).

[150] J. Shao and R. E. Baltus, "Effect of solute concentration on hindered diffusion in porous membranes," *AIChE Journal* **46,** 1307–1316 (2000).

[151] M. B. Albro, V. Rajan, R. Li, C. T. Hung, and G. A. Ateshian, "Characterization of the concentration-dependence of solute diffusivity and partitioning in a model dextran-agarose transport system," *Cell Mol Bioeng* **2,** 295–305 (2009).

[152] APP-Pharmaceuticals, "Prescription information for Iodopen Sodium Iodide (sodium iodide)," Package insert (2008).

[153] Guerbet, "Hexabrix," Package insert (2008).

[154] GE-Healthcare, "Prescribing information for Omniscan (gadodiamide)," Package insert (2010).

[155] Bayer-Healthcare-Pharmaceuticals, "Prescribing information for Magnevist (gadopentetate dimeglumine)," Package insert (2013).

[156] FDA, "Information for healthcare professionals: Gadolinium-based contrast agents for magnetic resonance imaging (marketed as Magnevist, MultiHance, Omniscan, OptiMARK, ProHance)," Web page (checked 26.3.2015) (2007).

[157] P. Dewachter, S. Castro, F. Zeitoun, S. Chollet-Martin, L. Gaillanne, M. Postaire, S. Pigneret-Bernard, and P. Nicaise-Rolland, "Immediate allergic reaction following intra-articular injection of ioxaglate confirmed by skin testing and flow cytometry-based basophil activation test," *Eur J Radiol* **74,** e27–e29 (2010).

[158] H. Lusic and M. W. Grinstaff, "X-ray-computed tomography contrast agents," *Chem Rev* **113,** 1641–1666 (2013).

[159] P. N. Bansal, R. C. Stewart, V. Entezari, B. D. Snyder, and M. W. Grinstaff, "Contrast agent electrostatic attraction rather than repulsion to glycosaminoglycans affords a greater contrast uptake ratio and improved quantitative CT imaging in cartilage," *Osteoarthritis and Cartilage* **19,** 970–976 (2011).

[160] C.-J. Qu, J. Rieppo, M. M. Hyttinen, M. J. Lammi, I. Kiviranta, J. Kurkijärvi, J. S. Jurvelin, and J. Töyräs, "Human articular cartilage proteoglycans are not undersulfated in osteoarthritis," *Connect Tissue Res* **48,** 27–33 (2007).

[161] NIST, "X-ray mass attenuation coefficients," Web page physics.nist.gov/PhysRefData/XrayMassCoef/tab3.html (2015).

[162] N. Blumenkrantz and G. Asboe-Hansen, "New method for quantitative determination of uronic acids," *Analytical Biochemistry* **54,** 484–489 (1973).

[163] D. E. Schwartz, Y. Choi, L. J. Sandell, and W. R. Hanson, "Quantitative analysis of collagen, protein and DNA in fixed, paraffin-embedded and sectioned tissue," *Histochem J* **17,** 655–663 (1985).

[164] QuickZyme-Biosciences, "QuickZyme Hydroxyproline Assay," Package insert (2015).

[165] Biocolor, "Blyscan Sulfated Glycosaminoglycan Assay," Package insert (2012).

[166] H. J. Mankin, H. Dorfman, L. Lippiello, and A. Zarins, "Biochemical and metabolic abnormalities in articular cartilage from osteo-arthritic human hips. II. Correlation of morphology with biochemical and metabolic data," *J Bone Joint Surg Am* **53,** 523–537 (1971).

[167] P. N. Bansal, N. S. Joshi, V. Entezari, M. W. Grinstaff, and B. D. Snyder, "Contrast enhanced computed tomography can predict the glycosaminoglycan content and biomechanical properties of articular cartilage," *OsteoArthritis and Cartilage* **18,** 184–191 (2010).

[168] B. S. Elkin, M. A. Shaik, and B. Morrison, "Fixed negative charge and the Donnan effect: a description of the driving forces associated with brain tissue swelling and oedema," *Phil Trans R Soc A* **368,** 585–603 (2010).

[169] K. A. M. Kulmala, H. M. Karjalainen, H. T. Kokkonen, V. Tiitu, V. Kovanen, M. J. Lammi, J. S. Jurvelin, R. K. Korhonen, and J. Töyräs, "Diffusion of ionic and non-ionic contrast agents in articular cartilage with increased cross-linking - Contribution of steric and electrostatic effects," *Med Eng Phys* **35,** 1415–1420 (2013).

[170] Z. K. Hawezi, E. Lammentausta, J. Svensson, L. E. Dahlberg, and C. J. Tiderius, "In vivo transport of Gd-DTPA2- in human knee cartilage assessed by depth-wise dGEMRIC analysis," *J Magn Reson Imaging* **34,** 1352–1358 (2011).

[171] E. R. Nightingale, "Phenomenological theory of ion solvation. Effective radii of hydrated ions," *J Phys Chem* **63,** 1381–1387 (1959).

[172] D. R. Lide, ed., *CRC handbook of chemistry and physics: A ready-reference book of chemical and physical data*, 86th ed. (CRC Press, Taylor and Francis, 2005).

[173] NIH, "ChemIDplus TOXNET Database," U.S. National Library of Medicine. Web page toxnet.nlm.nih.gov (2015).

[174] G. W. Greene, B. Zappone, O. Söderman, D. Topgaard, G. Rata, H. Zeng, and J. N. Israelachvili, "Anisotropic dynamic changes in the pore network structure, fluid diffusion and fluid flow in articular cartilage under compression," *Biomaterials* **31,** 3117–3128 (2010).

[175] N. S. Joshi, P. N. Bansal, R. C. Stewart, B. D. Snyder, and M. W. Grinstaff, "Effect of contrast agent charge on visualization of articular cartilage using computed tomography: Exploiting electrostatic interactions for improved sensitivity," *J Am Chem Soc* **131,** 13234–13235 (2009).

[176] P. N. Bansal, N. S. Joshi, V. Entezari, B. C. Malone, R. C. Stewart, B. D. Snyder, and M. W. Grinstaff, "Cationic contrast agents improve quantification of glycosaminoglycan (GAG) content by contrast enhanced CT imaging of cartilage," *J Orthop Res* **29,** 704–709 (2011).

[177] R. C. Stewart, P. N. Bansal, V. Entezari, H. Lusic, R. M. Nazarian, B. D. Snyder, and M. W. Grinstaff, "Contrast-enhanced CT with a high-affinity cationic contrast agent for imaging ex vivo bovine, intact ex vivo rabbit, and in vivo rabbit cartilage," *Radiology* **266,** 141–150 (2013).

[178] B. A. Lakin, D. J. Grasso, R. C. Stewart, J. D. Freedman, B. D. Snyder, and M. W. Grinstaff, "Contrast enhanced CT attenuation correlates with the GAG content of bovine meniscus," *J Orthop Res* **31,** 1765–1771 (2013).

[179] J. D. Freedman, H. Lusic, B. D. Snyder, and M. W. Grinstaff, "Tantalum oxide nanoparticles for the imaging of articular

cartilage using X-ray computed tomography: Visualization of ex vivo / in vivo murine tibia and ex vivo human index finger cartilage," *Angew Chem Int Ed* **53,** 8406–8410 (2014).

[180] R. J. Phillips, "The effect of surface charge distribution on hindered diffusion in pores," *J Colloid Interface Sci* **338,** 250–260 (2009).

[181] P. W. Atkins, *Physical chemistry*, 4th ed. (Oxford University Press, Oxford, 1990).

[182] P. A. Torzilli, "Effects of temperature, concentration and articular surface removal on transient solute diffusion in articular cartilage," *Med Biol Eng Comput* **31 Suppl,** S93–S98 (1993).

[183] A. S. Aula, J. S. Jurvelin, and J. Toyras, "Simultaneous computed tomography of articular cartilage and subchondral bone," *Osteoarthritis Cartilage* **17,** 1583–1588 (2009).

[184] L. N. M. Hayward, C. M. J. de Bakker, L. C. Gerstenfield, M. W. Grinstaff, and E. F. Morgan, "Assessment of contrast-enhanced computed tomography for imaging of cartilage during fracture healing," *J Orthop Res* **31,** 567–573 (2013).

[185] H. J. Yoo, S. H. Hong, J.-Y. Choi, I. J. Lee, S. J. Kim, J.-A. Choi, and H. S. Kang, "Contrast-enhanced CT of articular cartilage: experimental study for quantification of glycosaminoglycan content in articular cartilage," *Radiology* **261,** 805–812 (2011).

[186] M. J. Turunen, J. Töyräs, M. J. Lammi, J. S. Jurvelin, and R. K. Korhonen, "Hyperosmolaric contrast agents in cartilage tomography may expose cartilage to overload-induced cell death," *J Biomech* **45,** 497–503 (2012).

[187] T. Donath, F. Pfeiffer, O. Bunk, C. Grünzweig, E. Hempel, S. Popescu, P. Vock, and C. David, "Toward clinical X-ray phase-contrast CT: Demonstration of enhanced soft-tissue contrast in human specimen," *Invest Radiol* **45,** 445–452 (2010).

[188] A. Horng, E. Brun, A. Mittone, S. Gasilov, L. Weber, T. Geith, S. Adam-Neumair, S. D. Auweter, A. Bravin, M. F. Reiser, and P. Coan, "Cartilage and soft tissue imaging using X-rays: Propagation-based phase-contrast computed tomography of the human knee in comparison with clinical imaging techniques and histology," *Invest Radiol* **49,** 627–634 (2014).

[189] P. Julkunen, W. Wilson, H. Isaksson, J. S. Jurvelin, W. Herzog, and R. K. Korhonen, "A review of the combination of experimental measurements and fibril-reinforced modeling for investigation of articular cartilage and chondrocyte response to loading," *Computational and Mathematical Methods in Medicine* **2013,** ID 326150 (2013).

[190] M. Kazemi, Y. Dabiri, and L. P. Li, "Recent advances in computational mechanics of the human knee joint," *Computational and Mathematical Methods in Medicine* **2013,** ID 718423 (2013).

Tuomo Silvast

Contrast enhanced computed tomography of articular cartilage

Laboratory investigations on contrast agent molecular mass, charge, concentration and diffusion anisotropy

Diagnostics of early osteoarthritis is challenging with current clinical imaging techniques. This study investigated the potential of contrast enhanced computed tomography (CECT) to detect variations in cartilage composition and integrity. X-ray contrast between intact and degenerated cartilage and inverse relationship between diffusion rate of contrast agent and tissue solid content suggest that CECT is a promising technique for diagnostics of cartilage injuries and degeneration *in vivo*.

UNIVERSITY OF EASTERN FINLAND

BIOPHYSICS BONE AND CARTILAGE

Publications of the University of Eastern Finland
Dissertations in Forestry and Natural Sciences

ISBN: 978-952-61-1913-7 (printed)
ISBN: 978-952-61-1914-4 (pdf)
ISSN: 1798-5668
ISSN: 1798-5676 (pdf)